5-2014

Development of a Testing Platform for Secondary-Use Electric Vehicle Batteries as Community Energy Storage Systems

Thomas Benjamin Ollis
University of Tennessee - Knoxville, tollis@utk.edu

To the Graduate Council:

I am submitting herewith a thesis written by Thomas Benjamin Ollis entitled "Development of a Testing Platform for Secondary-Use Electric Vehicle Batteries as Community Energy Storage Systems." I have examined the final electronic copy of this thesis for form and content and recommend that it be accepted in partial fulfillment of the requirements for the degree of Master of Science, with a major in Electrical Engineering.

Fangxing (Fran) Li, Major Professor

We have read this thesis and recommend its acceptance:

Kevin Tomsovic, Yilu Liu

Accepted for the Council:
Carolyn R. Hodges

Vice Provost and Dean of the Graduate School

(Original signatures are on file with official student records.)

Development of a Testing Platform for Secondary-Use Electric Vehicle Batteries as Community Energy Storage Systems

A Thesis Presented for the
Master of Science
Degree
The University of Tennessee, Knoxville

Thomas Benjamin Ollis
May 2014

DEDICATION

To my parents, Paul and Sharon Ollis, my fiancé Rebecca Voeltz,

and all of my family and friends for their love and support.

ACKNOWLEDGEMENTS

I would like to thank my major professor, Dr. Fangxing "Fran" Li, for his knowledge and guidance throughout my time as a graduate student. I would also like to thank Dr. Michael Starke, Phil Irminger, and George Andrews from Oak Ridge National Laboratory (ORNL). Without their effort, support, and guidance, the research contained in this thesis would not exist. Thanks also to Kumar Prabakar for sharing his knowledge of the LabVIEW software and providing assistance in its deployment.

I would also like to thank Pablo Valencia, Peter Karlson, and Seelan Thambiappah from General Motors and Pablo Rosenfeld, Alex Goodson, and Sebastien Massin from ABB for providing the community energy storage unit and inverter, and also for all their technical support and knowledge throughout the testing, without which none of this would have been possible.

I would like to thank ORNL and CURENT for providing funding for my work on this thesis. Additionally, I would like to thank Dr. Kevin Tomsovic and Dr. Yilu Liu for being my committee members and reviewing my work.

ABSTRACT

Energy storage is quickly transforming from a commodity to a necessity for electric utilities. The peak demand on the electric grid continues to grow, requiring more sources of generation and upgrades to infrastructure. The variability of renewable generation sources, such as wind and solar, has created more uncertainty on the generation side of the electric grid. Energy storage represents one possible solution to mitigate the demand and uncertainty; however, energy storage systems have historically been too expensive to recoup their capital cost. More recently, research into electric vehicle batteries has brought their cost down and improved performance. As they continue to evolve and become more affordable, people are more likely to adopt electric vehicles as their primary mode of transportation. Eventually, the batteries will degrade to about 80 percent of their original capacity; at which time they are no longer viable to be used in a vehicle. Instead of dismantling these batteries, they can be repurposed as secondary-use community energy storage devices and used for grid applications.

This thesis examines the use of five Chevrolet Volt battery packs from General Motors repackaged by ABB with an interfacing inverter to perform real world tests on the viability of secondary-use electric vehicle batteries as community energy storage systems. Residential load profile predictions are used in conjunction with a programmable load bank and genetic algorithm optimization to test residential load factor control. A 14 kilowatt photovoltaic array is used to determine how effectively the unit smooths power fluctuations using neural network photovoltaic power predictions. Historical regulation signals from the Pennsylvania-Jersey-Massachusetts (PJM)

independent system operator (ISO) are used to demonstrate the performance of the unit while providing regulation services. The control, data routing, and hardware communication of each of these applications is done through a MATLAB graphical user interface built specifically for this project. LabVIEW is used as the data acquisition system.

Finally, the performance of the community energy storage unit is analyzed and presented to show the potential and limitations of secondary-use electric vehicle batteries to perform grid applications. Future works regarding life cycle analysis and economic practicality are discussed in the conclusion.

TABLE OF CONTENTS

LIST OF TABLES

LIST OF FIGURES

CHAPTER I
INTRODUCTION

1.1. Energy Storage Obstacles

Energy storage systems (ESS) have always appealed to power system engineers and energy storage manufacturers for their potential grid applications. In the 1880's, New York City used lead-acid batteries to provide night-time load on the electricity system, which was DC at the time [1]. Today, approximately 160 GW-hours of operational energy storage is installed on the United States electric grid, with 97.6% being pumped hydro ESS [2]. One such pumped storage plant is the Raccoon Mountain pumped storage station, owned by the Tennessee Valley Authority. The station can produce 1652 MW of power for 22 hours when completely full [3]. The station serves as one of the largest forms of hydroelectric power in the southeastern United States. The breakdown of energy storage by type across the U.S is shown in Table 1.1.

Table 1.1: U.S. operational energy storage capacity (in MW) [2].

Storage Type	***Total Power of Storage***	***Percentage of Total***	***Total Energy of Storage***	***Percentage of Total***
Pumped Hydro	6,240	95.4 %	155,986	97.6 %
Battery	133.5	2.0 %	158.8	0.1 %
Compressed Air	113.5	1.7 %	3,362	2.1 %
Thermal	47.7	0.7 %	347.9	0.2 %
Other	6.0	0.1 %	1.5	0.001 %

More recently, the focus of research on energy storage has moved away from large-scale pumped hydro towards smaller, less land restrictive forms of energy storage,

such as compressed air, thermal, flywheel, and battery energy storage. Large-scale pumped hydro typically has a large geographic footprint and can be heavily dependent on the landscape. The last pumped hydro station built in the US was in the 1980s, after which concerns over land and water usage severely restricted the deployment of more stations [1]. Meanwhile, technology has continued to advance on other forms of energy storage for use on the electric grid.

One major obstacle limiting the wide scale use of ESS is a high initial capital cost. According to the DOE/EPRI/NRECA 2013 Electricity Storage Handbook, the average capital cost for 8 lithium-ion ESS installations from 2010 to 2011 averaged $1,334 per kWh [1]. Meanwhile, in 2013 the average capital cost for an advanced combined cycle gas plant was $1,023 per kWh [4].

Because ESS are expensive, it is important to use them in applications which provide a large value to the owner. This way, the ESS will recover its initial cost quickly and become an asset and not a burden. Finding a single particular grid application which recovers the capital cost quickly is a difficult task [5]. Instead, if ESS can perform multiple grid applications, it is more valuable than if it could perform only one.

1.2. Applications for Energy Storage

In an electric grid, power must be generated as it is consumed. This requires the constant adjustment of the output power of generators to match the changing load. With energy storage, this is not necessarily the case. Energy can be absorbed when it is not needed and then discharged when it is needed. There are many potential grid applications

which take advantage of energy storage to make the electric grid more stable, efficient, and economical.

One application for ESS is the time shifting of renewable generation. Certain forms of renewable generation such as solar and tidal power will produce the most power during fairly predictable times. However, during these times the power might not be needed. In this scenario, the utility will be over-generating and will either need to sell energy or reduce the output of some generators. This can be seen clearly in Figure 1.1, where the power from photovoltaic panels reduces the load during the middle of day, then causes a rapid ramp up to the peak load when the panels' production begins to fall.

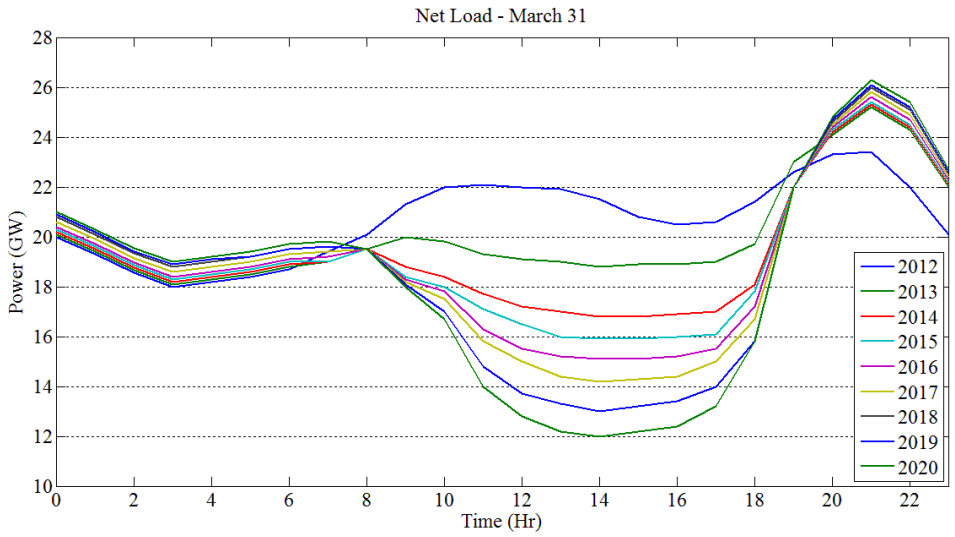

Figure 1.1: Duck Curve [6]

Using high energy forms of ESS, the energy from the renewables can be stored and provided to the grid when it is needed. This strategy prevents the utility from over-generating due to the renewable energy sources. A similar strategy for usage of ESS is

energy arbitrage. For energy arbitrage, energy is bought and stored when it is cheap and then sold when it is more expensive. This requires a similar type of ESS as generation shifting, and some units could perform both simultaneously.

ESS can also be used for peak shaving, where the ESS stores energy during times of low load and provides energy during times of high load. By having the ESS provide the peak load, the utility may not need to activate peaking generators, which are many times more expensive than other forms of generation. Reducing the peak may also allow the utility to avoid upgrading expensive equipment to handle the peak power level. Peak shaving also has potential for commercial and industrial applications. To avoid a high demand charge, a commercial or industrial customer can use ESS to provide the peak, as in [7]. This application requires ESS which can store large amounts of energy for many hours and then discharge over many hours.

Regulation is another potential grid application for ESS. Regulation from ESS primarily benefits the transmission system with increased reliability. When providing regulation, the output power of ESS will fluctuate based on a signal from a transmission operator. The signal from the transmission operator is based on the needs of the grid. If the system frequency dips, load exceeds generation and the transmission operator will likely request an increase in output power to maintain system stability. High power ESS are best suited for this application, as the net energy required for this type of service is typically low.

Many ESS generate power in DC. To interface with the grid, these ESS require a bi-directional inverter to convert the DC to AC. With the inverters for the ESS, it is possible to perform power factor control or reactive power support. The inverters can

either absorb or provide reactive power to move the power factor closer to unity. This presents value to large customers with loads which have a particularly bad power factor, as the customer can avoid bad power factor charges from the utility where typically a 0.95 leading or lagging limit is imposed. Also, by providing reactive power, the inverters can provide voltage support for long lines which absorb a large amount of reactive power. This helps to improve system stability and reduce losses resulting from having a low voltage and high current.

The final application considered here is uninterruptible power. In the case of a grid outage, ESS can provide power to customers until the grid is restored or until there is no more stored energy. This benefits the utility by allowing the continued sale of energy to customers even during an outage. This also benefits large or crucial customers such as hospitals by allowing them to continue their operation during the outage, activate backup generators, or shut down equipment in a controlled manner to prepare for total loss of power. The ESS does not have to benefit only one customer. In the case of a micro-grid, ESS can be used as a power source for a potentially large amount of customers. With appropriate amounts of ESS, a large micro-grid can be operated independent of the grid and remain stable.

1.3. Objectives

The use of ESS has many potential grid applications which offer utility savings and improved system stability. Currently, the use of ESS is increasing as technology advances and systems become more economical. One rapidly growing area of ESS is electric vehicles. Hybrid and fully electric vehicles are becoming more common on the

road due in part to increased fuel savings over the life of the vehicle compared to traditional gasoline vehicles. At the end of the useful life of the electric vehicle, the batteries contained in them are typically still useful for other applications. Multiple used electric vehicle batteries can be deployed in parallel by a utility as an ESS for grid services. The potential for penetration of secondary-use electric vehicle battery ESS increases as more electric vehicles leave the road. Having a large number of small ESS will allow individual systems to perform location-specific applications, while also giving the utility the ability to coordinate the units' dispatch to act as a generator. Before a utility is willing to invest in large amounts of energy storage, it must be clear that installing the storage will be economical. Therefore it is important to have large amounts of test data on ESS in real world applications to determine the criteria which make the storage profitable.

The objective of this thesis will be to investigate and test multiple grid applications on a physical secondary-use electric vehicle battery ESS. Each application will use a different control scheme to attempt to optimize the performance of the ESS. The results from the tests will provide useful data on how effective these battery units can be for individual grid applications. This analysis can later be scaled up to determine how to optimize the usage of the ESS to provide the most value to the owner.

1.4. Summary

This thesis will present controls, optimization, and testing data for a physical secondary-use electric vehicle battery energy storage unit. The results will show the real behavior of a single unit used for many different grid-related applications. Chapter 2 will

investigate different energy storage technologies, along with background on secondary-use batteries, community energy storage, and detailed descriptions of grid applications for energy storage. This chapter will also detail 2 significant algorithms used for optimization and prediction of various parameters. Chapter 3 defines the methods used for testing of the unit. It details the equations, controls, and experimental setup used to prepare for testing. Chapter 4 explains the results from simulations and long term testing of the unit. Chapter 5 presents the conclusion for the work contained in this thesis, as well as suggests areas for further study.

CHAPTER II
BACKGROUND

2.1. Types of Energy Storage

Many different forms of man-made energy storage exist today. Each form attempts to store either potential or kinetic energy for future use. The individual types of energy storage also store different forms of potential and kinetic energy, such as the energy from chemicals, gravity, electrical potential, thermal gradients, pressurization, and momentum. Storing a certain form of energy gives each type of energy storage its own unique characteristics. The benefits and drawbacks of various forms of energy storage will be briefly investigated in this section.

2.1.1. Traditional Batteries

A tradition battery stores potential energy in the form of chemical mixtures. These types of batteries have a positive (cathode) and a negative (anode) terminal. During discharge, electrons flow from the cathode to the anode, changing the energy from chemical to electrical. An example battery model showing how the chemicals interact in a lithium-ion battery can be seen in Figure 2.1. The direction of electron flow can be reversed to recharge some forms of batteries. The charging and discharging of a battery, referred to as a cycle, can be performed a finite number of times. After a certain number of cycles, the internal chemicals, catalysts, and cell walls degrade to a point at which the battery can no longer be used.

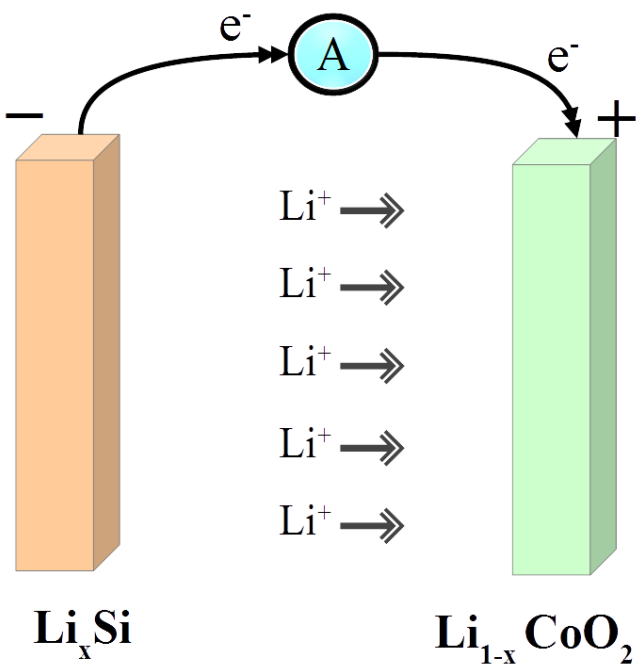

Figure 2.1: Lithium ion battery model [8]

Many different battery chemistries exist, with lead-acid, nickel-metal hydride, and lithium-ion being some of the most popular. Battery chemistry determines how a battery will perform in a given application. For example, a given battery chemistry may have a short lifetime or low efficiency, but also be very cheap. More expensive battery chemistries may have a longer lifetime and higher efficiency, but pose an environmental risk if the chemicals were ever to be released from the batteries. Table 2.1 compares some important operating characteristics for various battery chemistries.

Table 2.1: Battery chemistries and characteristics [9],[10]

Chemistry	*Efficiency (%)*	*Cost ($/kWh)*	*Cycle Life at D (cycles/%)*
Lead-Acid	75-85	80	1000/50
NiMH	65-85	350	3500/80
Li-Ion	90	315	4500/80
NaS	85	230	4500/90

Traditional batteries can serve a wide range of applications, due in part to their portability, ease of use, flexibility in supply power, and sizing ability. Batteries are simple to customize to a given application using different combinations of series and parallel batteries to provide different voltage and current levels. This makes batteries an attractive option for grid applications.

One major downside to battery energy storage is their capital cost. Because batteries are expensive, it is critical to find applications for batteries which provide the most benefit quickly. Environmental concerns are another downside to battery units. Because some batteries contain potentially toxic chemicals, it is important to take precautions in case of battery failure with chemical spill.

2.1.2. Flow Batteries

Flow batteries are similar to traditional batteries in that they use the potential difference between chemicals to generate a current. However, unlike traditional batteries, flow batteries have many moving parts. Chemicals stored in an electrolyte are pumped from tanks through tubes separated by a membrane. When a load is connected to the

membrane, electrons are exchanged between the chemicals, creating current flow to the load [10].

Flow batteries typically do not suffer from self-discharge because the chemicals are stored in separate tanks. Some forms are also capable of almost instantaneous output and can have a lifetime of around 10 years [1]. Because the chemicals are stored in tanks, large flow batteries can have very large tanks which take up a wide area. When decommissioned, some flow batteries have parts which have become toxic and must be disposed of carefully [1].

2.1.3. Pumped Hydro

Pumped hydro energy storage is the most prevalent form of man-made energy storage on the planet [11]. Energy is stored as gravitational potential energy by pumping water uphill from a source to a large reservoir where the water is stored. When the energy from the pumped hydro plant is needed by the utility, the water will be allowed to flow downhill to drive generators and create electricity.

One of the major benefits of pumped hydro energy storage is the sheer amount of energy which can be stored. The reservoirs where the water is stored are often quite large and energy dense, allowing the pumped hydro station to provide large amounts of energy for a long time span. Pumped hydro stations also have a very long lifetime, on the order of 50 to 60 years [1].

One of the advantages of pumped hydro energy storage can also be seen as a disadvantage. Pumped storage stations can store massive amounts of energy due to the fact that they often have large reservoirs. These reservoirs take up quite a bit of land and

are often expensive to purchase for the utility. Another major challenge is that it is difficult to find locations geographically suited to pumped hydro energy storage. Not all utilities have locations with large, high elevation reservoirs with nearby water sources. Pumped hydro stations are also immensely expensive initially, but their long lifetime help to recuperate the capital cost.

2.1.4. Ultra Capacitor

Ultra capacitors (UC), also known as super capacitors, are large capacitors which can store energy electrostatically in an electric field. Due to their simple construction, they have a very low internal resistance, high efficiency, and long lifetime. UCs can typically be cycled 1,000,000 times with no capacity loss [12]. UCs also have a very high power density, making them suitable for applications that require a fast response or high power for a short time.

Although UCs have a high power density, they have a very low energy density; much less than the other forms of energy storage mentioned here. To get the most value from UCs, they are often combined in parallel with ESS which have a high energy density. This configuration allows the UC to provide the fast power needs of the system and the other energy storage system to take care of the slower needs of the system.

2.1.5. Thermal

Thermal energy storage (TES) systems are used to store heat or cold to be used later as air conditioning or to generate electricity. Using deep wells or highly insulated containers (or both), TES systems can store thermal energy for a length of time ranging from nightly storage for use in the day (or vice versa), or seasonal storage for use in a

later season [13]. Considering that utility peak loads typically occur during times when large numbers of air conditioners are operating at once, TES could be quite effective at lowering the peak by providing hot or cold air to buildings. When used to generate electricity, TES can use energy sources such as concentrated solar or geothermal caverns to heat up a fluid and use that fluid and a heat exchanger to superheat steam to turn a turbine [13]. TES is a high energy type of storage, as it typically has a slower response to load. This is due to the time it takes for heat exchanges to occur, a necessary step in using TES for energy.

2.1.6. Compressed Air

Compressed air energy storage involves the use of a motor to pump air into a vessel for storage. These vessels can be small or ultra-large, depending on the application. When the energy is needed, the motor acts as a generator and is spun by the air as it escapes the highly pressurized vessel. The amount of power in or out of the system can be controlled with a valve on the vessel, making compressed air storage very flexible in terms of operation. Compressed air systems also have a very long lifetime (40 years) when compared to batteries, and efficiencies in the range of 75-80% [14].

One of the main drawbacks of compressed air storage is the low energy density of pressurized air when compared to the energy density of the water used in pumped hydro stations. Also, like pumped storage, it is difficult to put large scale compressed air storage stations exactly where they are needed due to geographical constraints.

2.1.7. Flywheel

Flywheel energy storage is one of the few forms of ESS which store kinetic energy as opposed to potential energy. A flywheel designed for energy storage is a large disk rotating at very high speeds with a very high moment of inertia, giving it a substantial amount of kinetic energy. To store energy, the rotational speed of the flywheel is increased, usually by a generator attached to the flywheel shaft. To release energy, the flywheel is allowed to drive the generator shaft, generating electricity but decreasing the flywheel rotational speed. Flywheels are typically used in high energy applications, primarily due to the fact that the stored energy is proportional to the square of the rotational speed.

To increase the maximum energy storage capacity of a flywheel system, either the moment of inertia or the rotational speed must be increased. As rotational speed increases, so do losses from friction. Mitigation of friction losses between the flywheel and the air requires that flywheels typically be stored in a vacuum. Even in a vacuum, flywheel losses exist in the mechanical bearings connected to the shaft [15]. As these bearings are replaced, it increases the cost of the system. Another cost consideration when looking at flywheels is safety in the case of failure. Most flywheels are designed to fail in a specific fashion; however flywheel containers must still be very strong and located underground in the case of catastrophic failure [15].

2.2. Secondary-Use Battery Energy Storage

Electric vehicles are quickly becoming more common on the road, partly because of advances in battery technology. Automobiles have a limited lifetime, and the

expectation is that the battery may outlive the vehicle. Once off the road, the batteries from the vehicles can either be dismantled and thrown out or repurposed as "secondary-use" batteries. The term "secondary-use" is used to describe energy storage (most often batteries) that have reached an objective lifetime in one application and moved to another application where the capacity of the energy storage system is still sufficient. In this case, the battery energy storage involves used lithium-ion batteries from electric vehicle batteries which have been reached the end of their useful life as vehicle batteries and must be repurposed or recycled [16].

There is a great deal of literature investigating the lifetime of lithium-ion batteries [17-21]. From the papers, it is clear that battery lifetime is heavily dependent on 3 parameters: the depth of discharge (DOD), the number of cycles, and the operating temperature. The DOD refers to how deeply the battery is discharged with respect to the total energy in the battery, normally represented as a percentage. The deeper the DOD, the shorter the life of the battery will be. Cycling refers to how many times the battery can be taken to a certain DOD before it can no longer perform. For example, a certain battery may last 1000 cycles at 80% DOD or 4000 cycles at 50% DOD. The last major parameter affecting lifetime is operating temperature. A temperature too high or too low will affect the chemical reactions within the battery and cause degradation. The relationship between temperature and cycling at 100% DOD can be seen in Figure 2.2. The data from Figure 2.2 comes from a test of automotive lithium-ion batteries performed in [22].

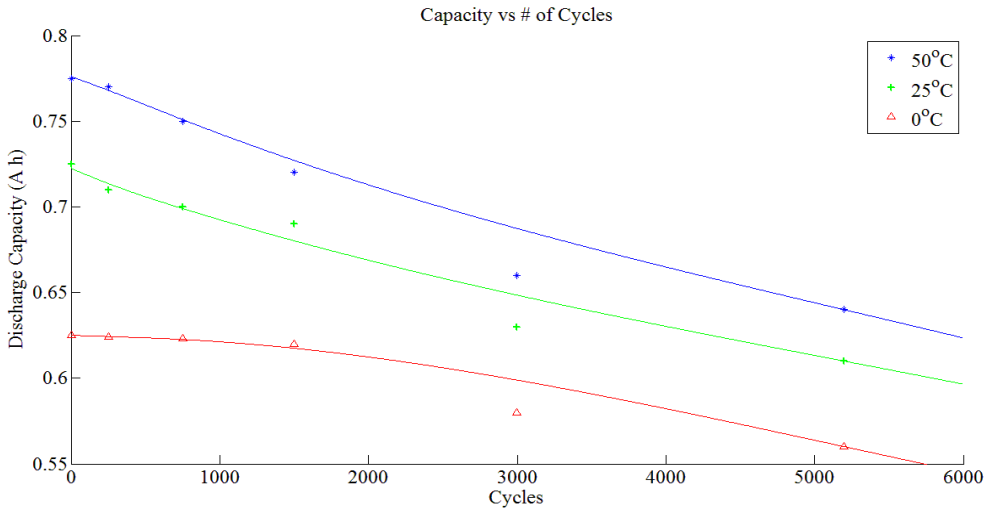

Figure 3.2: Capacity loss from cycling at different temperatures [22]

Electric vehicle batteries are typically deemed unfit for continued use after they lose 20% of their original capacity [23]. Lifetime for a Chevrolet Volt lithium-ion battery was estimated by the manufacturer to degrade by 20 to 30% after 8 years or 100,000 miles [24]. After this time, if the battery is removed from the vehicle it will still have 80 to 70% of its initial capacity. The remaining useful life can be used for grid applications such as community energy storage. By distributing secondary use batteries throughout the distribution grid, the individual batteries can perform local operations while the aggregate total of the batteries can act as their own generation unit [16].

2.3. Community Energy Storage Systems

Secondary use batteries have the potential to become useful for grid applications. Because batteries are more portable, energy dense, and easy to size compared to other forms of energy storage, they are popular candidates for Community Energy Storage (CES) systems. The primary focus for CES has been the delivery of services to groups of

homes. By distributing CES units throughout portions of the grid, the units can act as a generator when aggregated while also being able to perform more localized tasks [16]. Some applications for CES units which have been investigated in this thesis include renewable shifting, renewable smoothing, peak load reduction, reactive power support, uninterruptible power, and aggregated grid services.

2.3.1. Interconnection

CES units are typically not very large (~25 kW, 50 kWh), and so they are used to serve between 3 and 5 homes, depending on the loads present in those homes. As shown in Figure 2.3, CES units and the power electronics required to interface them to the grid are installed on the secondary side of the transformer. With this setup, the CES unit acts as a buffer between any renewables or loads and the grid.

After installation of a CES unit, the effect of load growth from charging of electric vehicles can be mitigated, potentially preventing the need for a transformer upgrade. This is possible if the CES unit can provide the peak load for the homes which it is connected to. Also, a disconnect switch between the transformer and CES unit allows the residential homes to be fed power from the unit in the case of system outage.

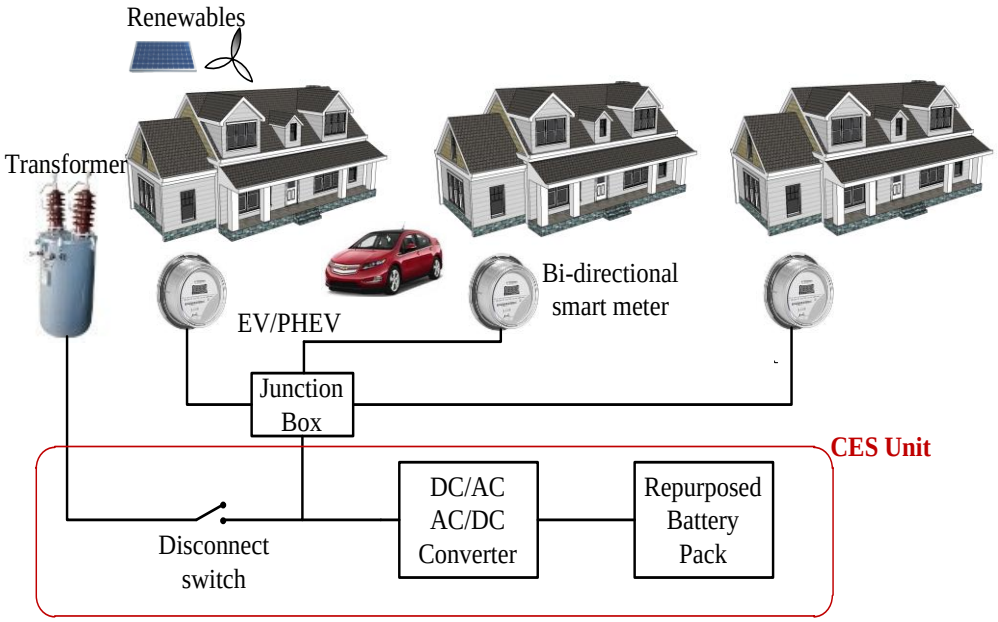

Figure 4.3: Community Energy Storage interconnection to residential homes

2.4. Applications

CES units are very flexible in that they can be used for many different applications by the owner. Applications can also change at any time based on the needs of the grid. The more tasks an energy storage system can perform for the grid, the more value it is to the grid owner.

2.4.1. Peak Shaving & Load Factor

During any given day, a utility operator monitors the system load and dispatches generators appropriately. Figure 2.4 shows an example of unit dispatch for one day with many different types of generators. The cheapest forms of generation are dispatched first, while the most expensive forms of generation are dispatched only as a last resort. Two critical times during a day for a utility include the valley and peak load times. During the

valley load time, the amount of load the utility must serve is at a minimum. To avoid over-generation, a utility must reduce output or completely shut down some of their generators or sell energy during the valley. Since it is normally less expensive for a generator to continue to run than to stop and restart, utilities benefit from a valley load level which allows cheap generators to operate all the time.

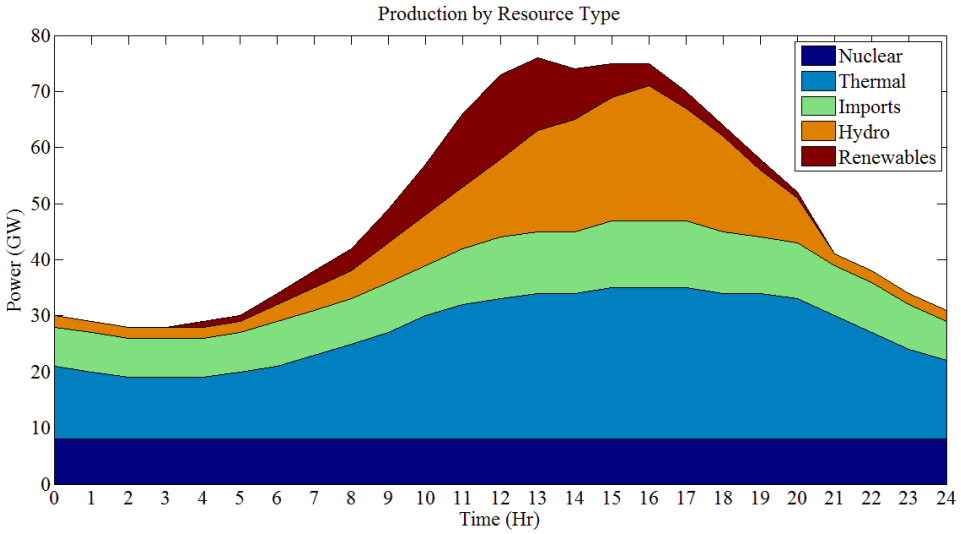

Figure 5.4: Example of generation usage for one day

The peak load time occurs when the load that must be supplied by the utility is at a maximum. This could require the utility to deploy most or all of its generation resources to meet the peak load. The generators used to supply the peak are the most expensive, so utilities benefit from a peak load level which does not require the use of the peaking units. An example of increasing generation cost with increasing load can be seen in Figure 2.5.

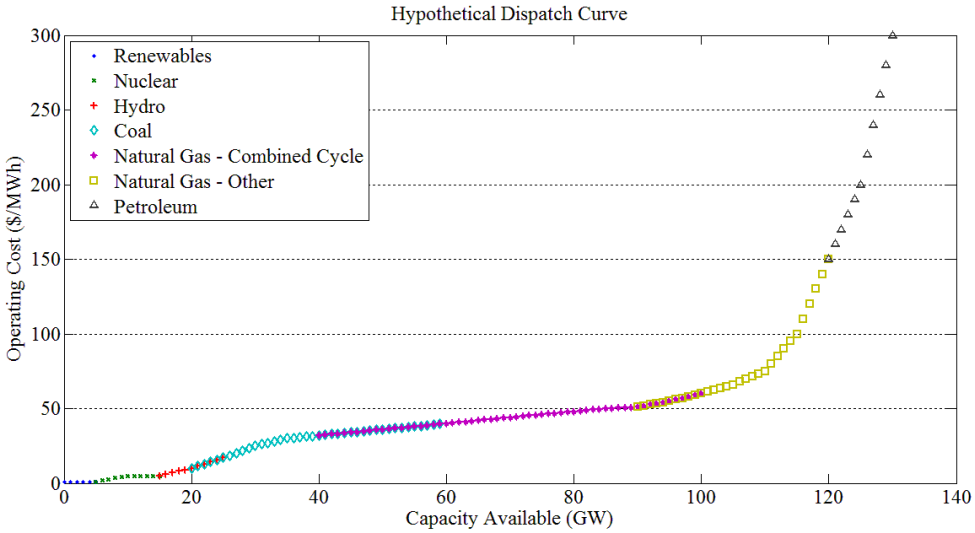

Figure 6.5: Example of generation cost vs load [25]

Peak shaving allows a utility to store energy in an ESS during times of valley load and then use that energy during times of peak load. When the price of storing energy becomes cheaper than the price of reducing generation, utilities will store energy until the ESS can no longer store energy or it is no longer marginally profitable to store energy. Energy is the cheapest during the valley load times. By storing energy instead of reducing generation, the valley load is raised, potentially keeping some generating units online. Then, when the price of generating energy with the ESS is cheaper than generating energy with another form of generation, the utility will generate with the ESS until it either runs out of energy or is no longer profitable. Figure 2.6 shows how an example load profile from [26] can be manipulated through peak shaving. When the energy in the ESS is dispatched, it effectively lowers the system load by serving loads which would have been served by increasing generation or buying power from another utility. This

process of saving energy from one point in the day until another is also referred to as energy shifting.

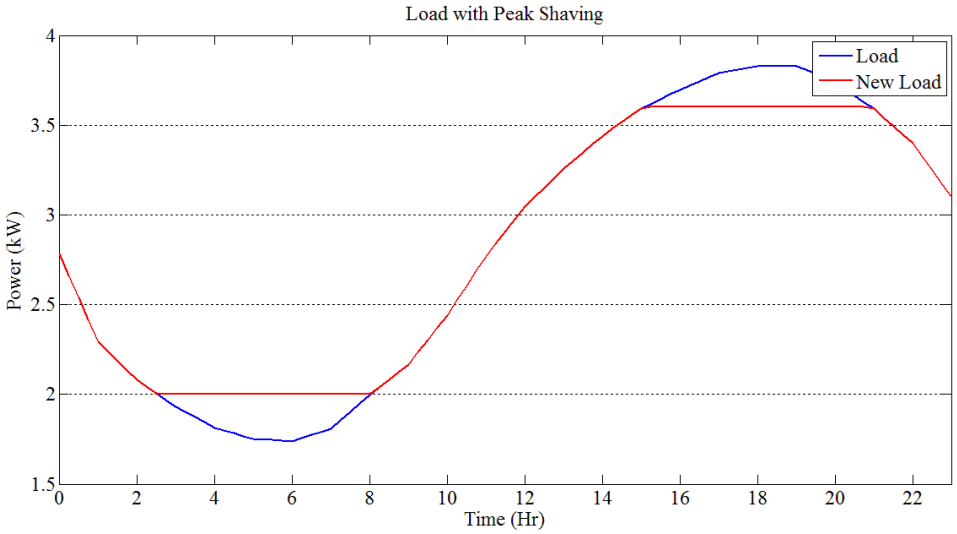

Figure 2.6: Typical load profile with peak shaving

Another form of peak shaving exists on the customer level. On top of their normal electricity rate, large customers typically pay a demand charge. This demand charge applies to the peak load for the customer over a given time period, usually a month. The demand charge can be many times higher than the normal electricity rate, and represents one of the major costs to large customers, such as industrial plants. For example, using the GSA rate structure from Knoxville Utilities Board [27], the customer is required to pay a demand charge of $12.73 per kW every 30 minutes on the demand over 50 kW. If the demand from the customer is 50 kW for 5 days a week, except for 1 hour a day when the demand is 75 kW, the customer must pay a demand charge on the 2 30-minute periods of 75 kW demand every day for that month. If the month has 4 weeks, then the

total demand charge comes to $12,730 for their load during that month. Thus, it is advantageous for large customers with a demand charge to keep their peak load low. Had the customer in the above example owned an ESS capable of providing the 25 kW peak load for the hour of peak demand, it could have avoided paying the $12,730 demand charge that month. The ESS may only be used for that hour during the day, but depending on the demand charge it could pay for itself in just that a few months.

A modified version of peak shaving called load factor control is another potential application for ESS. Load factor is a ratio relating the peak load to the average load over a given period of time. A load which is constant would have a load factor of one, whereas a load containing peaks would have a load factor closer to zero. The benefits of a high load factor include load predictability, near flat demand curve, and deferral of upgrades in some cases. Figure 2.7 contains an example of a load profile after load factor control.

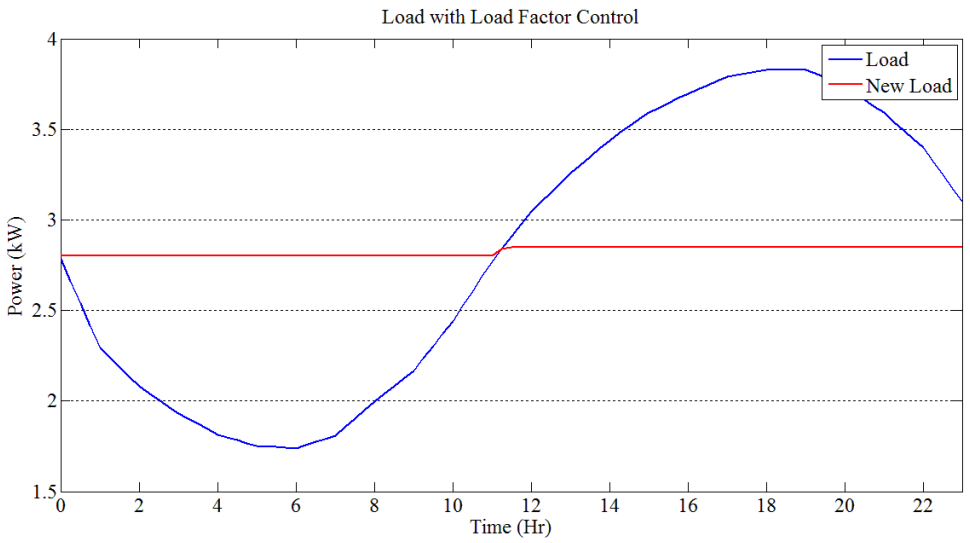

Figure 2.7: Typical load profile with load factor control

During load factor control, an ESS will operate almost constantly by either charging to raise the load level or discharging to lower the load level. This is in contrast to peak shaving, where there is one large charge and discharge cycle during the day. Because of this difference, it is important to monitor the state of charge (SOC) of the ESS at all times. The SOC is a percentage representing the amount of available energy left in the ESS with 100% SOC representing the maximum energy capacity. The SOC can quickly reach a high or low level during load factor control, limiting the performance of the ESS. A high SOC prevents the batteries in the ESS from absorbing more power, and a low SOC makes the batteries incapable of discharging more power. Either of these scenarios would be detrimental to the effectiveness of the load factor control, making load prediction a valuable tool.

2.4.2. Renewable Integration

Penetration of distributed renewable generation sources on the electric grid brings a host of benefits and problems. Issues such as variability of power supply and off-peak generation are investigated in this section.

2.4.2.1. Renewable Smoothing

Uncertainty continues to be one of the leading problems associated with renewable generation. Traditional forms of generation are highly controllable and predictable. An operator can adjust the output power of some forms of generation easily. Renewable generators do not have this luxury, as the fuel source (i.e. wind, irradiance) is typically uncontrollable and dynamic. A cloud passing over a solar farm can drop the

output power by 40% in a few seconds. Figure 2.8 shows an example of the fluctuations in output power for a group of solar panels.

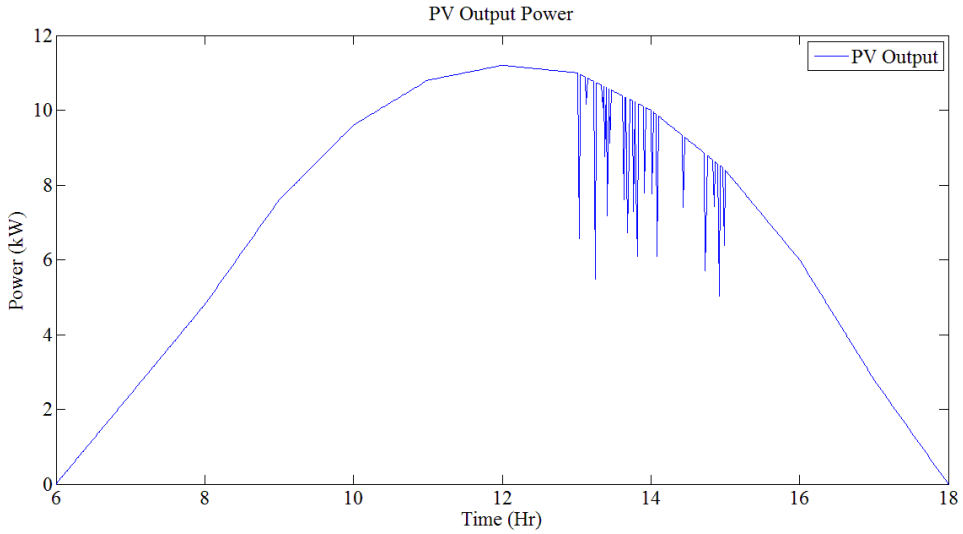

Figure 2.8: PV output fluctuations

Large swings in output power can wreak havoc on a power system, causing large voltage transients on the grid. Many studies have been done on the impact of PV penetration on the grid [28-31]. Spinning reserve can be used to mitigate transients; however large solar or wind farms could require multiple generators to act as reserves, which can become expensive over time. As PV penetration increases, more reserves will be required to maintain system stability.

ESS can be used to replace spinning reserve as a backup to renewable generation. System operators at utilities use weather forecasts to predict how much power should be generated at any given time by the renewables. If the renewable generation exceeds or falls short of the prediction, ESS can provide the difference and bring the net generation

back to the prediction. Figure 2.9 shows the output power of a group of solar panels after an ESS is used for smoothing. This relieves the need for spinning reserve as a backup. Also, since most ESS can provide power almost instantaneously, the grid will see only a small fluctuation in output power from the renewables before the ESS can compensate.

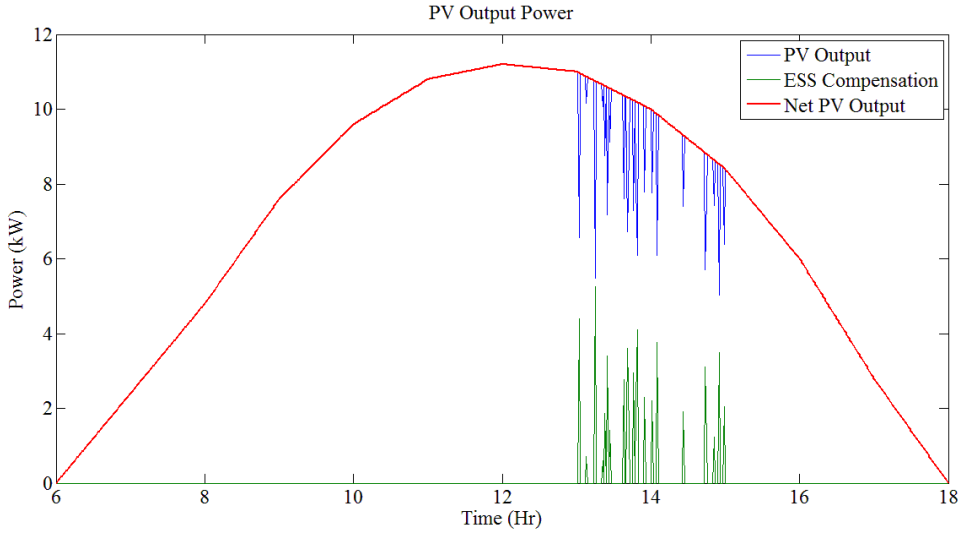

Figure 2.9: PV output with ESS smoothing

2.4.2.2. Renewable Shifting

Another issue associated with renewable integration is the need for renewable shifting. Because the fuel source for renewable energy is generally uncontrollable, renewable generation stations have the potential to produce a large amount of power when it is not needed, or no power at all when it is most needed. For a utility, the peak load on the system typically occurs between 3 – 5 pm. However, the maximum solar irradiance for the day typically occurs between 11 am – 1 pm. During this time frame, solar panel output power is at the maximum for the day. After 1 pm, the irradiance begins

to decline along with the output power of the panels. Because the peak in generation does not coincide with the peak in load, there is a possibility of having an excess amount of energy early in the day and a deficit of energy later in the day. As renewable penetration increases, this scenario becomes increasingly probable, as shown in Figure 1.1. It can be seen the power output of the renewables creates a potential for over generation, followed by a very fast ramp up to the peak load. The ideal performance of renewable generation would have the panels produce peak power during the peak load times. This can be done through the use of ESS.

An ESS can store energy from a renewable source during its time of maximum production and save that energy until the grid needs it the most. This allows a utility to avoid potential over generation early in the day and to have extra power to supply the peak. For solar power, shifting typically involves storing energy for only a few hours. In the case of wind power, the peak output could occur at any time during the day, so the ESS must be able to store energy for a longer period of time. Either way, an ESS allows the power from a renewable generation source to be used when it is most needed instead of when it is produced.

2.4.3. Regulation Services

Regulation services account for small, fast changes in load and generation which cannot be captured in energy markets that operate on 5 to 15 minute transactions. They are used to balance the load and the generation quickly to avoid deviations from the nominal frequency. Once a generator has agreed to provide regulation to a utility, the utility sends the generator a regulation signal so it knows how much regulation to

provide. Because loads are constantly being turned on and off by customers, the regulation signal constantly increases and decreases to accommodate the load changes. Over the course of the regulation period, the net energy used by the regulating generator should be equal to zero or very close. This means that on average, the output of a generator providing regulation services and the same generator not providing regulation services is the same.

Spinning generators were originally designed to perform regulation on the electric grid. However, because of the inertia stored in spinning generators, it is difficult to adjust the output power quickly. CES units, on the other hand, have the ability to change output power in a few seconds. With a faster response than traditional spinning generators, CES units could offer a tighter control on matching the generation and load. Since individual CES units are many times smaller than traditional generators, they do not have much of an individual effect on the system. However, when multiple CES units are aggregated together, they can act as a large generator and provide regulation services on par with larger, more traditional generators.

Signals for regulation services typically come in two forms: fast and slow. Fast regulation signals are sent to units which can provide power very quickly, such as battery or UC units. Slow regulation signals are reserved for units which have a slower ramp rate, such as gas turbines, and cannot change their generation as quickly as other generation units. Both these signals tell the generator exactly how much power to provide at a given time. Figure 2.10 shows an example of a fast and a slow regulation signal from a utility.

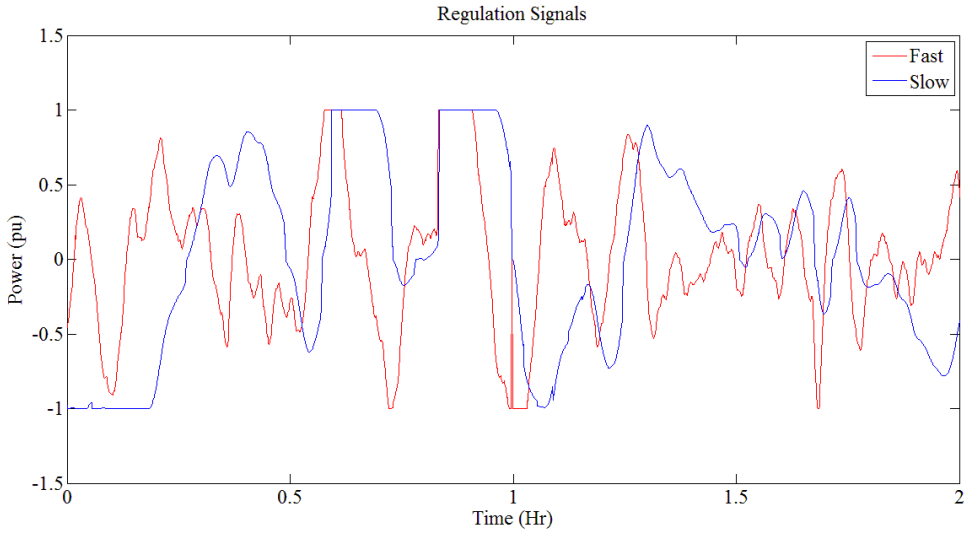

Figure 2.10: Regulation signals from a utility

2.4.4. Power Factor & Voltage Support

Power factor control for a load is another important application for any inverter connected ESS tied to the grid. Most large customers with a poor power factor are subject to a power factor charge from the utility they purchase from. Consider a large customer with rate structure SGSB from Knoxville Utilities Board [27]. The customer must pay a charge of $1.46 per kVAR for every kVAR which makes the power factor less than 0.95 lagging. The power factor charge applies for every 30-minute period in which the power factor drops below 0.95 lagging. If the customer has a real power demand of 5 MW and a reactive power demand of 2.42 MVAR, the power factor can be calculated as 0.9 lagging. For the same real power demand, the reactive power demand would have to be 1.65 MVAR to have a power factor of 0.95 lagging. If the customer operates at 0.9 lagging for 8 hours a day, 5 days a week, and 4 weeks a month, the power factor charge would be

$359,744 for that month. The charge is quite expensive, but can be mitigated through the use of an inverter connected ESS. The inverter can absorb or provide reactive power to the grid to raise the power factor and avoid the power factor charge. In the case of the above example, an inverter connected ESS capable of providing 770 kVAR could save the customer $359,744 per month, which could pay for the ESS quickly.

Power factor correction works particularly well in tandem with applications which serve load. By providing both the real and reactive power that a load requires with ESS, the grid effectively sees less or no load at the point beyond the ESS. Since the load is reduced, equipment ratings can be lowered, which saves the utility on upgrades and capital cost.

Providing reactive power support with ESS connected inverters also increases the local system stability. On a radial distribution network, the line voltage drops as you get further from the substation due to losses in the lines. By injecting some real and reactive power at points along the line, the voltage can be maintained or even boosted by inverter connected ESS. This allows the utility owning the line to avoid under voltage situations in times when the line is heavily loaded. It also reduces losses in the lines. A higher voltage means that less current can be sent for the same amount of power. Because losses are proportional to the current squared, a higher voltage reduces losses.

2.4.5. Islanding

ESS also allow for the creation of "islands" during loss of grid power. By disconnecting from the grid after an outage, an ESS can provide power to any loads connected to it. Hopefully, the ESS could provide power until such a time as the grid

power can be restored. The customer would never lose power in this scenario, allowing the utility to sell energy even during an outage. In the case of micro-grids, the ESS would act as a major source of generation and regulation for the micro-grid. If for some reason it became necessary for a micro-grid to become an island, an appropriate amount of ESS could regulate the micro-grid frequency and provide for the connected loads until such a time as the grid connection is restored.

2.5. Algorithms

2.5.1. Genetic Algorithm

Genetic algorithm (GA) is a simulation tool designed to find the optimum solution to complex or highly nonlinear problems by imitating the process of natural selection. GA begins with an initial population of potential solutions based on a fitness function and a constraint function which are specified by the user. The initial population of individuals is then evaluated based on how close each parent is to an optimal solution. Some individuals in the population which are far from the optimal solution will 'die off' or 'mutate' into a new solution. Other parents which are close to the optimum will pass to the next generation, combine to form an 'offspring' solution, or mutate. This process of selecting the most and least fit individuals repeats itself for every generation as in Figure 2.11. After enough generations have passed, the non-optimal solutions will have died off, and only the optimal solutions will remain. As more generations are simulated, the individuals have more opportunities to create the most optimal solution. However, more generations lead to a longer simulation time, so accuracy must be balanced with simulation time.

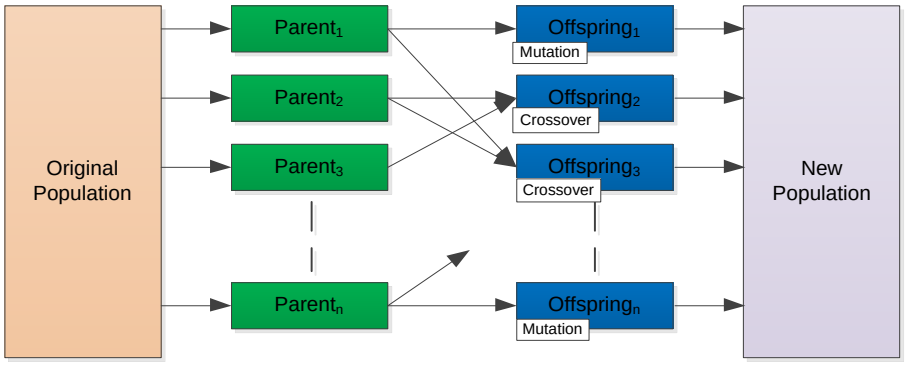

Figure 2.11: Genetic algorithm flowchart

2.5.2. Neural Networks

A neural network (NN) is a simulation tool designed to predict outputs and perform pattern recognition for highly nonlinear systems. NN are based off of the biological central nervous system, using many small nodes or 'neurons' in parallel to mimic brain function. Many neurons are connected together and adjusted based on network training data. The training data contains the input variables to the system, as well as the output(s) desired for control. During the training, the network adapts to the training data and arranges the nodes so that prediction and pattern recognition are possible for new, untrained data. This is useful for predicting the output of highly complex systems, and also for identifying which variables are important to a simulation.

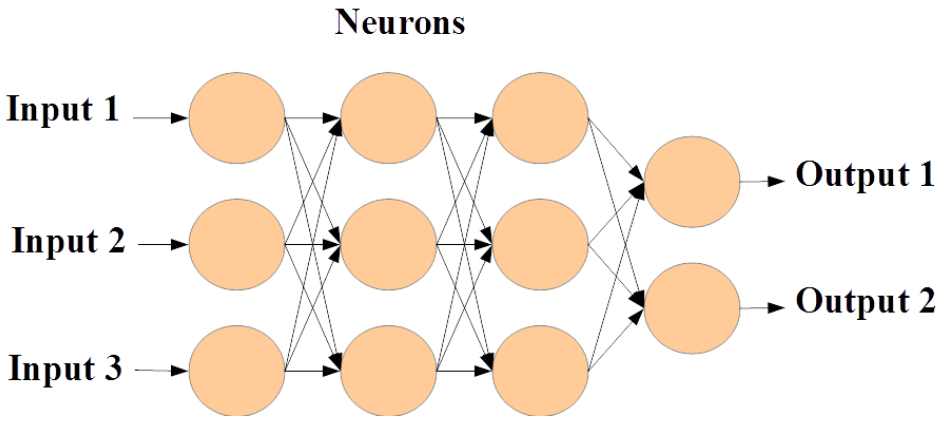

Figure 2.12: Neural networks

An accurate NN prediction is dependent on good training data. If there is too little training data, then the NN will not be able to make the proper connections between nodes and the predictions will be inaccurate at best. If there is too much training data, then the NN prediction will also be inaccurate, as the node connections will begin to overlap and detail will be lost.

CHAPTER III
METHODOLOGY

3.1. Equations and Theory

3.1.1. Battery Model

To better understand how the CES unit performs under various circumstances, a battery model was developed for simulation. Many battery models exist [32-36], but the developed model contains elements specific to the physical CES unit used for testing. The primary battery model parameters include the round trip efficiency including auxiliary losses and the state of charge (SOC) of the CES unit.

The round trip efficiency of the CES unit measures the percentage of energy stored in the battery which can later recovered for use in an application. The portion of energy which cannot be recovered is attributed to losses in the inverter and battery, and also to the auxiliary load in the CES unit. The auxiliary load represents necessary loads within the CES unit, such as the battery management and thermal management systems. To find the efficiency, the grid power is measured at the two points shown in Figure 3.1.

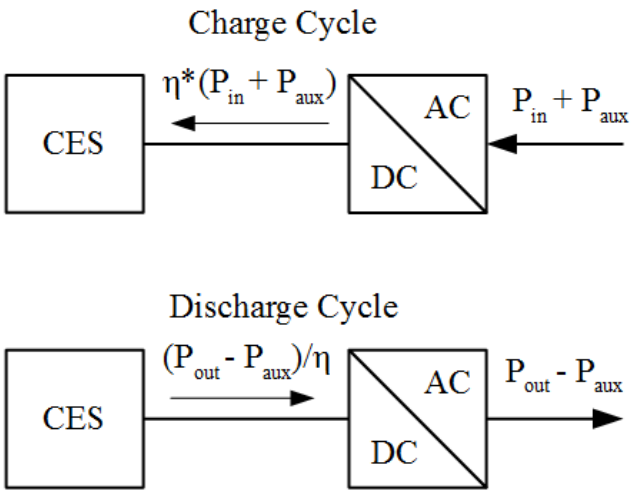

Figure 3.1: Charge-discharge cycle for efficiency calculation & SOC

From Figure 3.1, the round trip efficiency of the CES unit is defined in (3.1), where P_{out} is the power the grid sees from the battery, P_{in} is the power the grid injects into the battery, P_{aux} is the auxiliary load of the unit, t_1 is the charging time, and t_2 is the discharge time.

$$\eta = \frac{\int_0^{t_1} P_{out}(t)dt}{\int_{t_1}^{t_2} P_{in}(t)dt + P_{aux} * t_2} * 100\% \leftrightarrow SOC_0 = SOC_{t_2} \tag{3.1}$$

This equation is true when the SOC of the CES unit is the same before and after the charge/discharge cycle. In reality, the efficiency and auxiliary load will change depending on the amount of current through the inverter and the ambient conditions, so average values are used in the model.

The SOC is represented by a percentage and relates to the energy contained in the system. This is often defined as the actual energy currently in the system over the rated energy the system can store. The SOC can be expressed as (3.2), where E is the energy stored in the CES unit and E_{max} is the maximum energy which can be stored in the unit.

$$SOC = \frac{E}{E_{max}} * 100\% \quad (3.2)$$

As the CES unit operates, the SOC provides a window into the available energy and will typically increase with charging and decrease with discharging, although temperature and other factors are often used to understand the actual available energy in the storage medium. The SOC is monitored to ensure that the CES unit never exceeds a maximum or minimum energy threshold. The SOC after a time *t* during battery charging can be found with (3.3). The SOC during battery discharging can be found with (3.4).

$$SOC = SOC_{t=0} + \eta * \frac{\int_0^t P_{in}(\tau)d\tau}{E_{max}} * 100\% \quad (3.3)$$

$$SOC = SOC_{t=0} - \frac{1}{\eta}\frac{\int_0^t P_{out}(\tau)d\tau}{E_{max}} * 100\% \quad (3.4)$$

With the previous 4 equations, a model for the CES unit was constructed in software for the simulation of different applications for energy storage.

3.1.2. PV Model

Literature regarding PV modeling is abundant. The PV model used in this thesis was developed by Villalva [37]. This model was chosen because of the amount of information and components it considers. The model estimates the output power of a PV module considering solar irradiance, temperature, and an interconnected voltage. The power assumed produced by the PV model is at maximum power point (MPP). This is the highest point on the power/voltage curve of the PV panel. This assumption is often valid, as many of the interconnected inverters utilize maximum power point tracking (MPPT) to maximize solar energy production. Figure 3.2 shows the circuit diagram of the model.

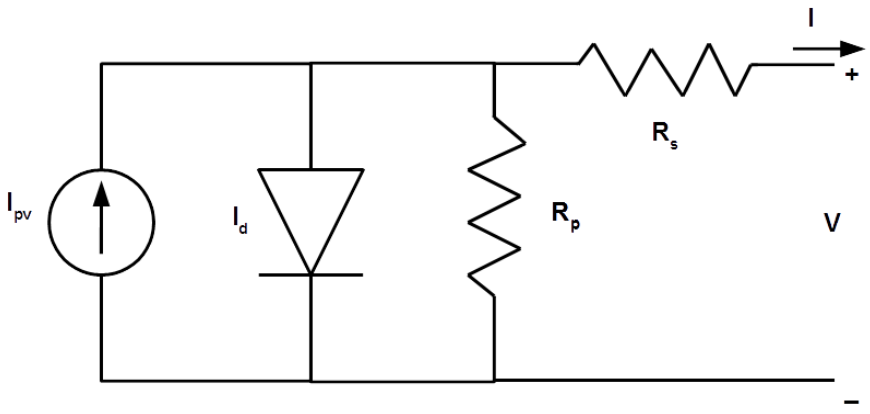

Figure 3.2: PV equivalent circuit

The current out of the PV module can be expressed as (3.5), where I_{pv} is the photovoltaic current, I_0 is the diode saturation current, V is the module voltage, V_t is the thermal voltage, R_s is the series resistance, R_p is the parallel resistance, and a is the diode constant.

$$I = I_{pv} - I_0\left(e^{\frac{V+IR_S}{aV_t}} - 1\right) - \frac{V+IR_S}{R_p} \tag{3.5}$$

The photovoltaic current can be found with (3.6), where I_{pvn} is the nominal PV current, K_I is a coefficient relating current and temperature change, T is the measured temperature in °C, T_n is the nominal temperature in °C, G is the measured solar irradiance in W/m^2, and G_n is the nominal solar irradiance in W/m^2.

$$I_{pv} = \left(I_{pvn} + K_I(T - T_n)\right) * \frac{G}{G_n} \tag{3.6}$$

The diode saturation current is given in (3.7), where I_{scn} is the nominal short circuit current, V_{ocn} is the nominal open circuit voltage, and K_v is a coefficient relating voltage and temperature change.

$$I_0 = I_{scn} + K_I(T - T_n) * \left(e^{\left(\frac{V_{ocn} + K_V(T - T_n)}{aV_t}\right)} - 1 \right)^{-1} \quad (3.7)$$

The thermal voltage for the diode is given by (3.8), where N_s is the number of cells in series in the module, k is the Boltzmann constant, and q is the charge of an electron.

$$V_t = \frac{N_s kT}{q} \quad (3.8)$$

The series and parallel resistance can be calculated using the method in [37]. The voltage in Figure 3.2 is incremented from zero to V_{ocn} to determine the current and power curves for the model, as seen in Figure 3.3 and Figure 3.4, respectively.

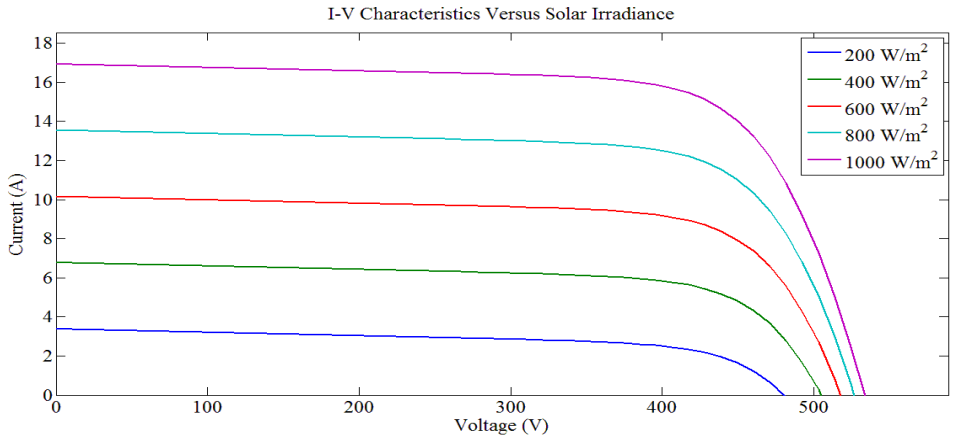

Figure 3.3: PV current characteristic

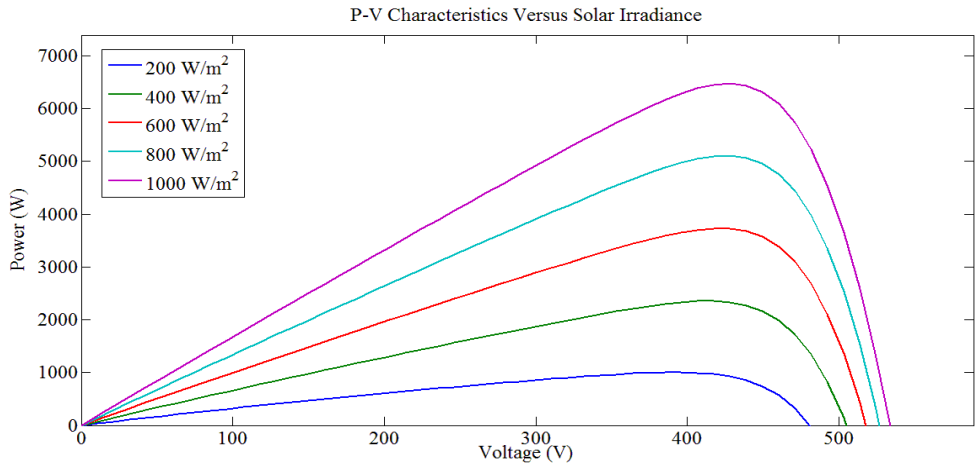

Figure 3.4: PV power characteristic

With the defined PV equations, simulations on PV output can be performed with irradiance and temperature data.

3.1.3. Residential Load Model

In a real world application, CES units are used primarily on the distribution side of the grid because of their small size. Thus, to maximize the CES units' value, it is important to understand how the residential loads fed by the CES units behave on any given day. The method used to model residential loads for use in testing the CES unit was designed by Johnson and is explained in [38]. The residential simulation tool (RST) produces residential load predictions on a 1 second or 1 minute time scale. The RST predicts the loads utilizing models of the household on the appliance level and the behavior of the home occupants. Occupant behavior data was gathered from the American Time Use Survey to create statistical models of how residents interact with loads within the home. Markov Chain Monte Carlo method is used to probabilistically determine the load for a home given the home size, appliances, number of occupants,

occupant work habits, day of the week, ambient temperature, and various other parameters. A simple Markov Chain is shown in Figure 3.5. The Markov Chains in the RST are much more complicated, and change depending on the time of day.

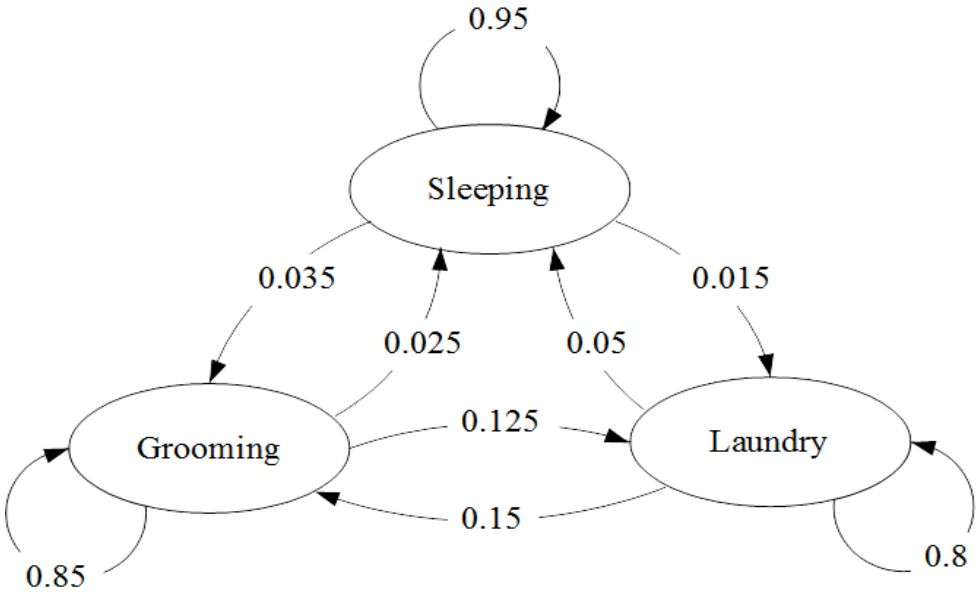

Figure 3.5: Example Markov Chain

3.2. Applications & Controls

3.2.1. PV Prediction and Control

Simulating PV smoothing first requires predicting the PV output for the day being examined. Since PV output prediction is a complex problem, a neural network (NN) approach based on temperature, sun angle, time of day, and cloud cover is used to simulate the irradiance curve for the day. The NN must be first trained to relate the real temperature data, cloud cover data, sun angle, and time of day to real irradiance

measurements. The irradiance can then be inserted into the PV model to estimate the power output.

The irradiance and power measurements are collected by the PV inverters in delimited files, which are then imported into the NN. The temperature data is imported from the Weather Underground website [39], which collects data from a weather station near the PV panels. The cloud cover forecasts are collected from the Canadian government website [40]. The website publishes 48 hours of cloud cover prediction images in 1 hour increments for most of North America for astronomical purposes. With these images, the cloud cover percentages for any point on the image can be found by comparing the color of the point in question to the key on the image. The resolution is not ideal, but this approach does provide a rough window into the available solar irradiance on an hourly time scale. Once the 24 hours for the simulation day have been analyzed for cloud cover, the cloud cover percentages are imported into the NN simulation for training.

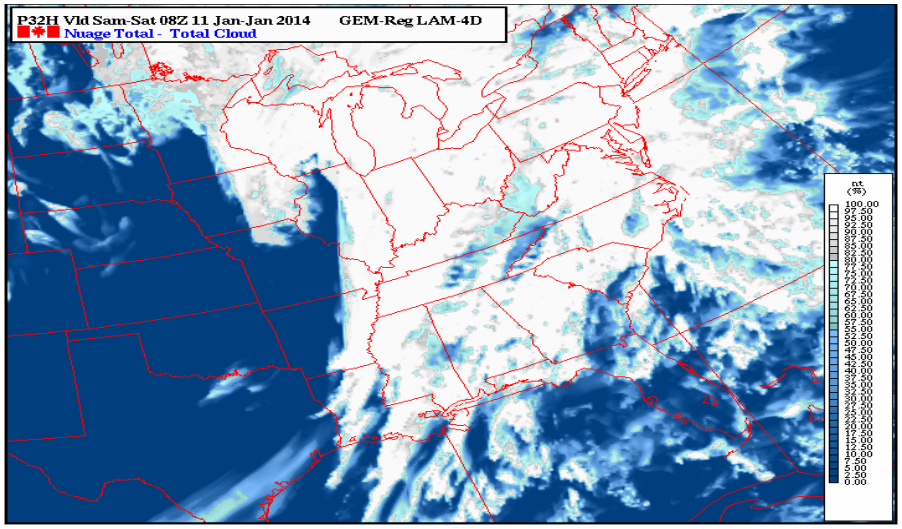

Figure 3.6: Cloud cover image from [39]

As more days of training data are collected, the NN prediction accuracy has seen improvements. The neurons in the network adjust their connections with increasing amounts of training data and 'learn' to associate certain temperatures, cloud cover percentages, and solar angles to levels of irradiance seen by the PV array. For the purposes of the PV smoothing application, approximately 21 days of data are trained by the NN before making the first prediction.

Once the network is trained with historical data, it is ready to predict the irradiance for the current day using the temperature and cloud cover data for the day. The temperature and cloud cover data can be collected from [39] and [40], respectively, and fed into the NN to predict the irradiance. With all the data, the NN produces a predicted irradiance for every hour in the day. The irradiance is then used as input to the PV model, which then outputs the predicted PV power for the day on a one hour resolution. The complete prediction process can be seen in Figure 3.7. The output power data is interpolated down to the second level used as the base for PV smoothing.

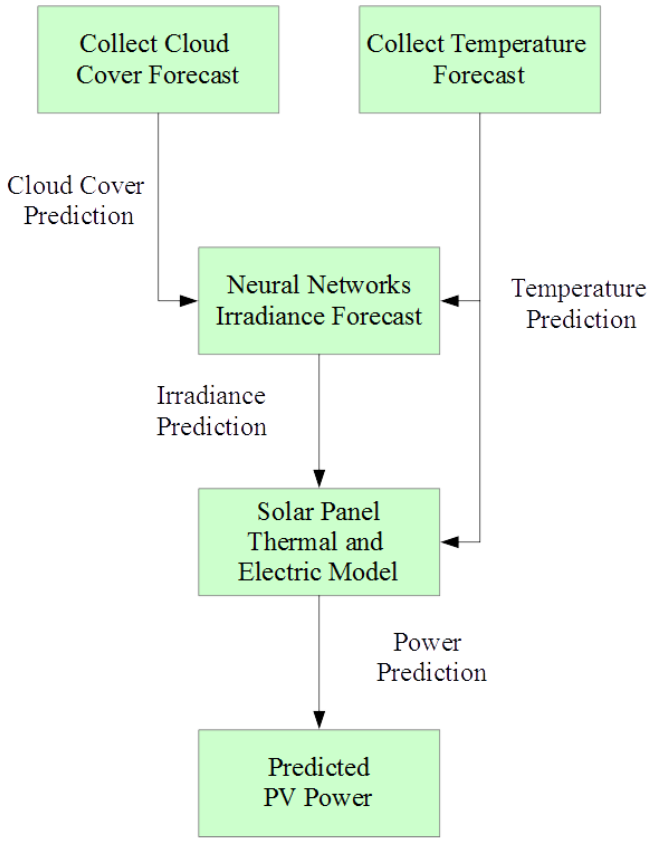

Figure 3.7: Complete approach to PV forecast

The curve produced by the NN represents the combined output power expected from the two modules in the PV array. As with any predicted output, there is always the possibility of errors between the real and the predicted output. For this application, the CES is used to compensate for the error and minimize it. By measuring the output power of the array, the compensation power needed from the CES can be calculated with (3.9), where P_{pred} is the predicted PV output power and P_{pv} is the actual PV output power.

$$P_{batt} = P_{pred} - P_{pv} \tag{3.9}$$

However, in the real case the power out of the inverter will most likely not be identical to the requested power because of losses between the battery and the grid. To

counteract this effect, a proportional integral (PI) controller is used to ensure that the correct amount of power is provided or absorbed by the CES unit.

The power needed from the CES unit is the difference between the predicted PV power and the actual PV power. The PV smoothing controller input is the error between the CES needed output and the CES actual output. This error is stored as the proportional error, and also integrated over the total time the controller has been active and stored as the integral error. The proportional and integral gains are tuned to best compensate for PV fluctuations, which often happen quickly as shadows due to cloud cover and other anomalies pass over the surface of the PV modules. Thus, the proportional gain is set to be large compared to the integral gain so that the PI controller would have a fast response time to these quick fluctuations. A diagram of the controller can be seen in Figure 3.8.

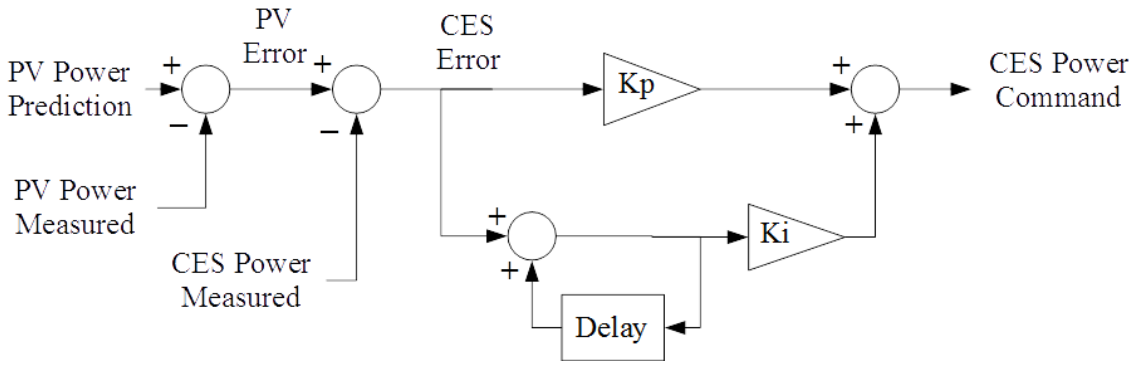

Figure 3.8: PV smoothing controller

3.2.2. Load Factor Prediction & Control

Performing a load factor simulation requires a residential load curve to flatten, a battery model to consider limitations, and a genetic algorithm (GA) optimization to obtain an optimal result.

To create the residential load profile, the RST is used. First, three homes are defined by specifying the occupants and the loads within the individual homes. Detailed parameters are available in Table A.1 of the appendix. Each home is simulated individually and then aggregated at the end of the simulation. The RST requires the ambient temperature and irradiance as input parameters, as certain parameters such as heating and cooling loads are heavily temperature dependent. The temperature and irradiance data are collected during the PV smoothing simulation, therefore the same data can be passed to the RST for the residential load simulation. The RST then produces the 24 hour load profile for the load factor simulation.

Once the load profile is obtained, the search begins for the optimal placement of set points which return the largest load factor. Load factor is defined in equation (3.10), where t_0 is the load profile start time, t is the end time of the time period, and L is the load profile for one day.

$$lf = \frac{\frac{1}{t-t_0}\int_{t_0}^{t} L(\tau)d\tau}{\max_{t_0 \to t} L} = \frac{average\ load}{peak\ load} \tag{3.10}$$

From (3.10), it can be seen that for a perfectly flat load profile, the load factor will be unity. In practice, a load factor of unity is nearly impossible, but load factors greater than 0.9 are achievable. A typical residential load profile has a load factor between 0.10 and 0.15 [41]. This load factor changes significantly throughout the year, mostly due to

increased heating and cooling in the winter and summer. With the right control scheme and CES, the load factor can be improved significantly.

To control the load factor of the residential load profile, a high and a low set point will be defined such that any load level above the high set point will be provided by the battery unit and any load level below the low set point will be absorbed by the battery unit. This relationship is expressed in (3.11), where P_{ESS} is the total power in or out of the ESS (negative is power in, positive is power out), L is the total load (Watts), and *hs* and *ls* are the high and low set points (Watts), respectively.

$$P_{ESS}(t) = \begin{Bmatrix} L(t) - ls, & L(t) < ls \\ 0, & ls \leq L(t) \leq hs \\ L(t) - hs, & L(t) > hs \end{Bmatrix} \tag{3.11}$$

The selection of the set points is critical to the effectiveness of the control. If the set points are far apart, then there will be a large dead band between them in which the battery unit does nothing. This decreases the battery unit's value as it is not providing any benefit to the grid. This also causes the load factor to move away from unity. If the set points are close together but set too high or too low, then the battery unit will move towards one of its SOC limits and possibly not be able to control the load factor. These scenarios are demonstrated in Figures A.1 through A.3.

Deciding the optimal locations of the high and low set points is a nontrivial problem which is quite difficult to solve by hand, so this work employs GA to determine the locations. The population size used for the optimization was chosen to be 300 individuals. This means that at the beginning of the first generation, GA creates 300 different pairs of set points to be tested. The pairs of set points are mostly random, aside from a constraint specified in the call to the algorithm which requires that the high set

point be larger than the low set point. After GA evaluates the fitness function with all 300 pairs of set points, the pairs which provide the most optimal results create an offspring pair, which is very similar to the parent pairs. Similarly, pairs which provide non-optimal solutions die off or mutate into a new pair. Once all offspring and mutations are completed, the optimization moves to the next generation. The maximum generation size was set to 30 generations. For these settings, GA will evaluate the fitness function 9000 times with different high and low set point pairs. The evolution of the optimum set points can be seen in Figure 3.9.

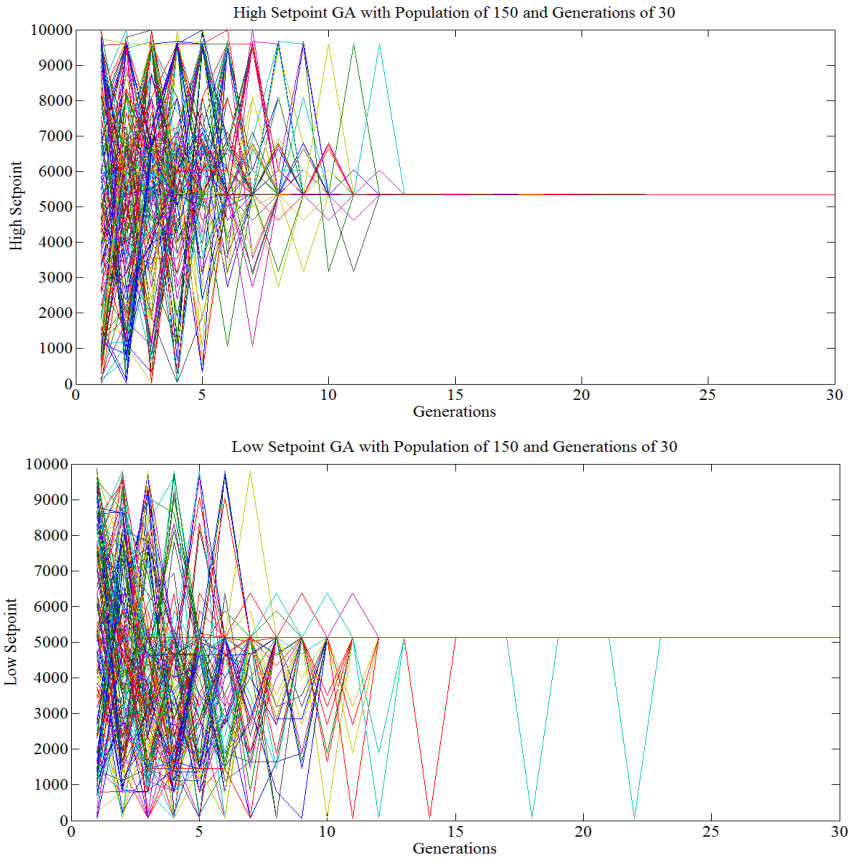

Figure 3.9: GA set point convergence

The fitness function for the GA was designed to accept the 24 hour residential load profile from the RST on a 1 minute time step and calculate the SOC and required battery power for each minute in the day based on the high and low set points. At the end of the day, the fitness function determines the load factor for that day using (3.10).

Pairs of set points which produce a load factor close to unity are more likely to pass on to the next generation. Built into the fitness function are constraints and penalties which influence which set point pairs are passed to the next generation. One such constraint penalizes pairs which cause the SOC of the battery unit to exceed 75% or drop below 30% at any time during the simulation. This constraint makes sure that there is never a time during the day where the unit cannot charge or cannot discharge. Another constraint penalizes pairs which cause the SOC of the battery unit to be outside of the range 45% - 55% at the end of the day. If the SOC were to be outside of this range at the end of the day, it would adversely affect the amount of energy available for control on the next day. The battery unit should be able to run optimally every day in order to maximize its value.

Once all generations have been completed, GA returns 300 pairs of set points and their corresponding load factors. These results are multiple different optimum solutions, but with slightly different set points, load factors, and ending energy. Once these solutions are returned, the solution which best fits the situation can be chosen by the user based on which optimum is most appropriate. For this paper, the solution with the highest load factor was chosen for testing.

In order for the CES unit to appropriately compensate for loads outside the band between the high and low set points, a fuzzy logic based PI controller was designed. This

controller first checks to see which of three possible states the load is currently operating in: greater than the high set point, less than the low set point, or between the high and low set points. For loads above the high set point, the input to the controller is the error between the grid power and the high set point. For loads below the low set point, the input to the controller is the error between the low set point and the grid power. For loads between the set points, the input to the controller is the error between the grid power and the load power. For loads not between the set points, the grid power measurement is used to calculate the error instead of the load power measurement because the end goal of this application is to flatten the load profile seen by the grid, so the grid power should be the target control measurement.

The PI controller is the same for all three scenarios described above, except for the input. For the load factor application, the control is most effective when the grid power can be moved to one of the set points as quickly as possible. However, a quick response often results in an overshoot past the desired set point. For small changes in load power, the overshoot is not very severe. But when the change in load power is large, this can result in a huge spike in grid power caused by the overshoot from the controller. From (3.10), it can be seen that a large spike in power will affect the load factor severely by increasing the value in the denominator. To avoid this, the PI controller gains were tuned so that there was no overshoot but with a longer settling time. This way, the large peaks from overshoot are avoided at the expense of the control taking more time to reach steady state. Figure 3.10 shows a diagram of the load factor controller.

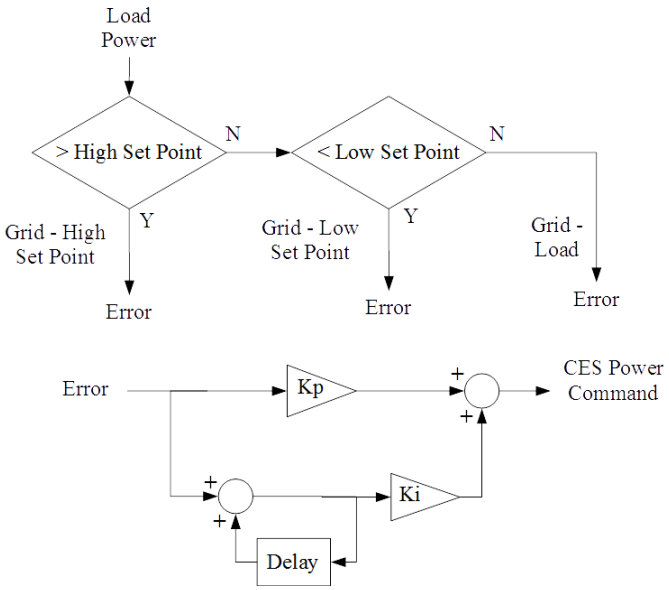

Figure 3.10: Load factor controller

3.2.3. Regulation Services Controls

Regulation services can be simulated utilizing an artificial regulation signal from a utility. For this simulation, fast and slow test regulation signals were obtained from the PJM website [42]. These test signals represent real regulation signals used by PJM in the past. The signals are in per unit, and were interpolated to give them a two second resolution.

Instead of directly sending the signal to the CES unit, the signal is given a bias of ±12 kW, or ±0.5 pu. This bias was applied because the inverter has a minimum power output, creating a dead band around zero in which no control or compensation can be done. By biasing the signal by half of the total output power of the CES unit (12 kW), more resolute control can be applied to the signal while sacrificing some control

bandwidth. Figure 3.11 shows the new control regions. Note that the dead band can be adjusted for the inverter, so the dead band shown is not necessarily the real dead band.

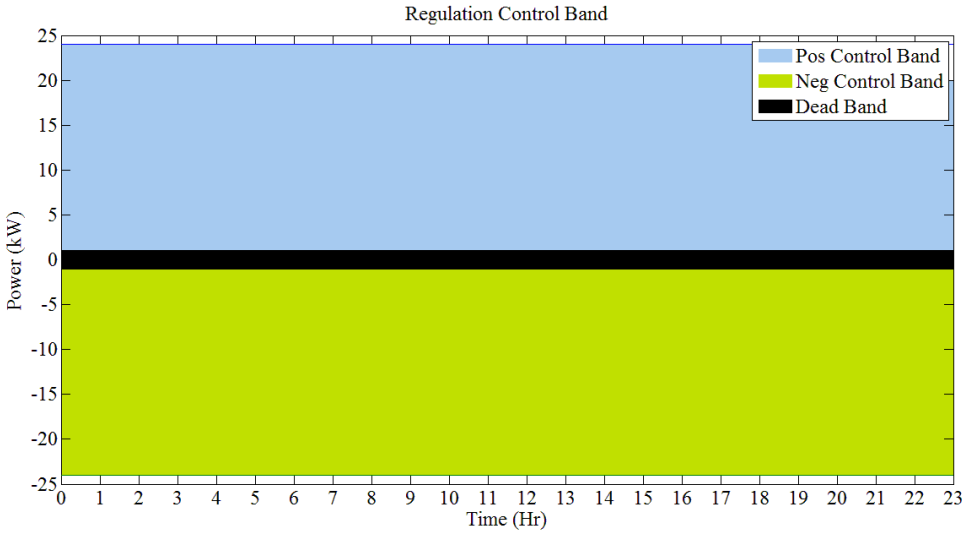

Figure 3.11: Regulation bandwidth

Because of the added bias, the unit will be either constantly discharging or charging, depending on if the bias is positive or negative, respectively. This could quickly cause the CES unit to go into a state where the SOC is near either its low or high limit. To accommodate this possibility, the sign of the bias is changed when the SOC reaches either a low or high threshold set in the controller. Once the bias changes signs, the CES will continue to provide regulation, just in the opposite charge/discharge state it was in before reaching the threshold. This should keep the net energy of CES unit close to zero while providing regulation services.

3.3.Experimental Setup

3.3.1. Equipment

General Motors (GM) and ABB provided Oak Ridge National Lab (ORNL) with a 25 kW (50 kWh) rated power battery energy storage unit. The battery unit consists of five secondary-use Chevrolet Volt lithium-ion battery packs connected in parallel. The unit also includes heating and cooling elements for thermal management and an on-board computer which runs the battery management system (BMS) to ensure proper operating conditions and monitor for errors. To interface the battery unit to the electric grid, ABB provided an inverter connected in split-phase to ORNL. The inverter monitors the connection to the battery unit and also stores important data which can be accessed via a communication port in the inverter control board. Together, the inverter and battery unit form the secondary use community energy storage unit used for the testing outlined in this document. The unit was installed at the Distributed Energy Communications & Controls (DECC) lab at ORNL.

Figure 3.12: Community Energy Storage Unit

In order to simulate residential load profiles, ORNL purchased a 36 kW 3 phase programmable load bank from NH Research. The load bank is capable of receiving a simulated load profile and mimicking the profile in real impedances. The simulated profile specifies the duration of each load level (as short as one cycle), the power factor for that load level, and the individual phase load. The load bank is capable of operating in current, resistance, and power control modes. For our tests, the load bank was operated in the power control mode, as this mode allows the load bank to change its resistance depending on the voltage it sees, keeping the power level constant. Since the inverter for the CES unit is connected in split-phase, only two phases of the load bank were used, bringing the total possible load from the load bank down to 24 kW, which is also the maximum power output of the CES unit.

Figure 3.13: Programmable load bank and disconnects

PV panels from Hanwha were installed on the roof of the DECC lab so testing could be done on PV smoothing using the CES unit. The maximum power output of the PV array is 13.4 kW. The array is split into two groups of panels, with one group facing south and the other group facing north. This was done because of the space and loading requirements of the roof of the DECC lab. Each of the two groups is connected to its own SMA inverter (two total), along with two sensors (four total) on the roof which record solar irradiance, ambient temperature, and solar cell temperature. The data collected by the sensors is used to train the neural network which predicts the irradiance levels seen by the PV panels.

Figure 3.14: Photovoltaic panels on lab roof

The CES unit, load bank, grid, and PV panels were metered to provide data for both control and result verification. The CES unit and inverter provided their own metering which could be accessed via the communication channel on the inverter. The load bank had metering points on each phase for current and voltage, for a total of four measurements. The grid had two metering points, one on each phase for the current. The grid voltage was assumed to be identical to the load voltage, because they are tied together. Each of the two PV inverters provide split-phase power, so the output of the inverters were metered as follows: one measurement per phase of current and voltage, making a total of four metering points per group and eight total PV metering points. This culminates in 14 total metering points. These measurements were collected through BNC cables to a National Instruments Compact Rio field-programmable gate array (FPGA) running LabVIEW software. The incoming analog data is processed by the software and used to calculate and store 30 different system parameters until the user requests the data.

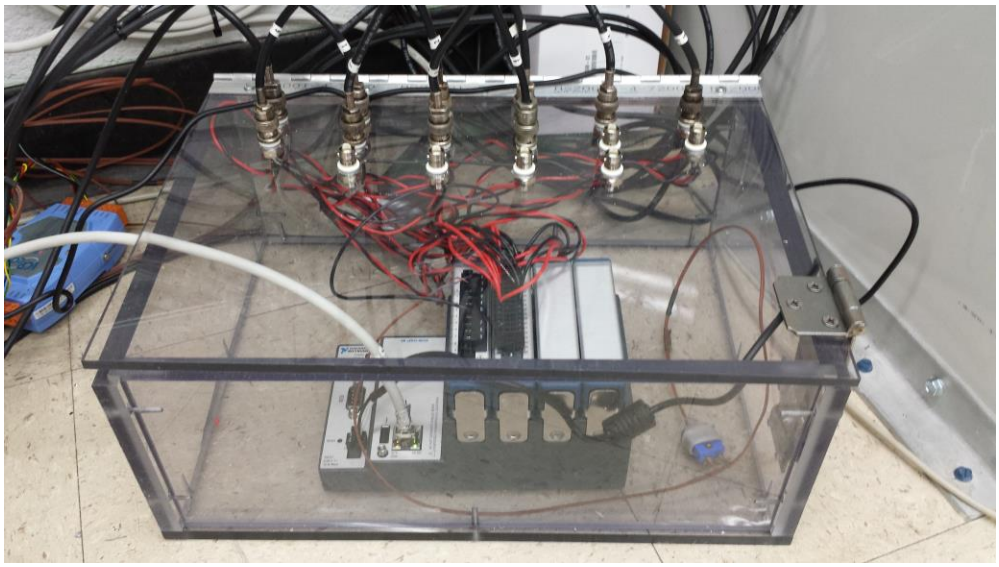

Figure 3.15: FPGA enclosure for data acquisition

3.3.2. Software

The CES unit and FPGA are interfaced through MATLAB, which serves as the primary interface for operation of the unit. All of the controls, communications, data logging, and error handling are done through a MATLAB graphical user interface (GUI), seen in Figure 3.16. The GUI is the backbone of the testing of the CES unit. During testing the GUI displays any and all important data in an easy to read manner which makes it simple for an operator to analyze performance with minimal delay. The operator can activate the inverter from inside the lab, and either send manual power commands to the unit or activate one of the many control schemes described in section 3.2 and allow the unit to run on its own. During operation, the GUI automatically logs crucial data every one to two seconds. This data can be moved to a separate MATLAB program which formats the data for analysis.

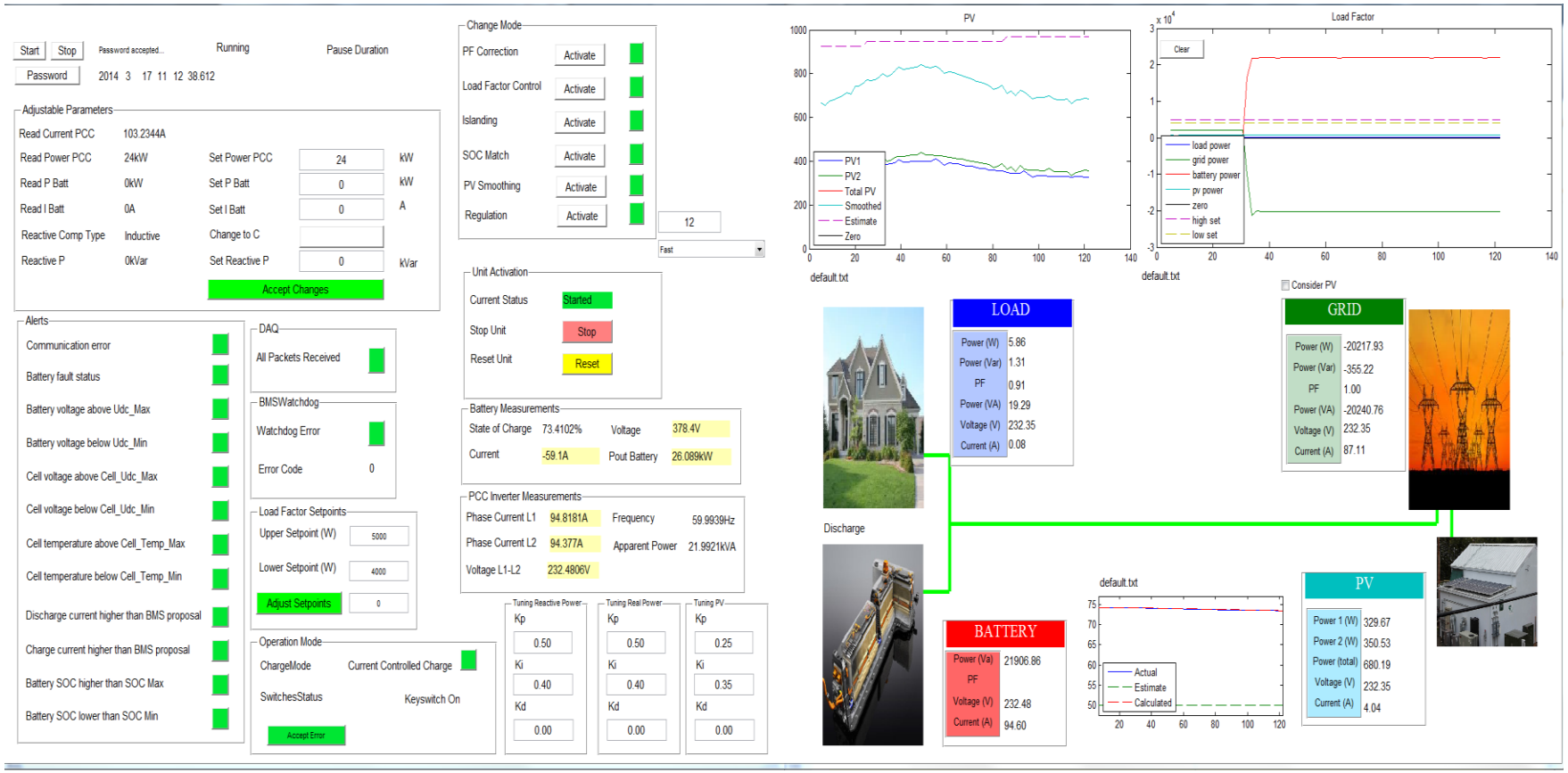

Figure 3.16: MATLAB GUI

The FPGA is programmed with LabVIEW software for importing, formatting, and calculating the data to be sent to the main MATLAB GUI. The block diagram in Figure 3.17 shows the block diagram used to process the measurements coming into the FPGA. By loading the software on the FPGA, it can run independent of a computer. This allows the FPGA to take in measurements and perform calculations very quickly while leaving the main computer free to perform control actions. Once the FPGA receives a signal from the GUI, it sends all of the collected measurements to the GUI for use in controls and data analysis.

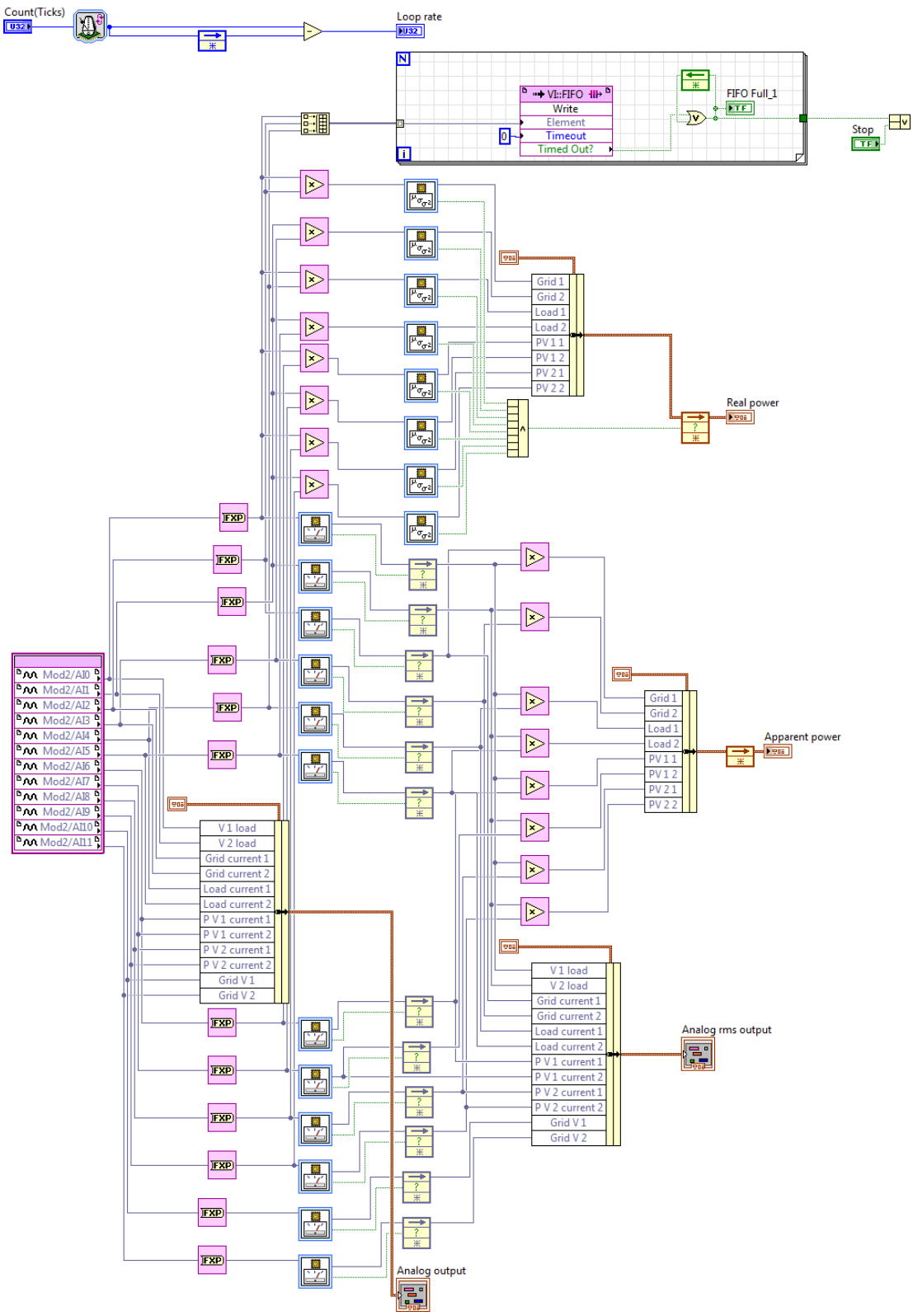

Figure 3.17: LabVIEW diagram

3.3.3. Communication

GM provided their own BMS to monitor the state of charge, voltage, temperature, and various other parameters inside the battery enclosure. The BMS sends critical data to the inverter where it is stored in registers along with essential inverter measurements and parameters. The inverter is connected to a computer inside the lab through a serial to RS-485 adapter located on the inverter control board. By sending commands through this communication channel, the computer can access the registers within the inverter control board and allow a user to gather all the reported data to analyze the performance of the inverter and unit. Some registers on the control board can have data written to them, allowing a user to control the real and reactive power output of the unit. Communication to the inverter is performed in MATLAB through Modbus protocol. Considering MATLAB has no built in Modbus functionality, all of the data formatting and transmitting had to be designed based off of existing Modbus applications. Figure 3.18 shows the process necessary for successful Modbus communication through MATLAB over a serial cable.

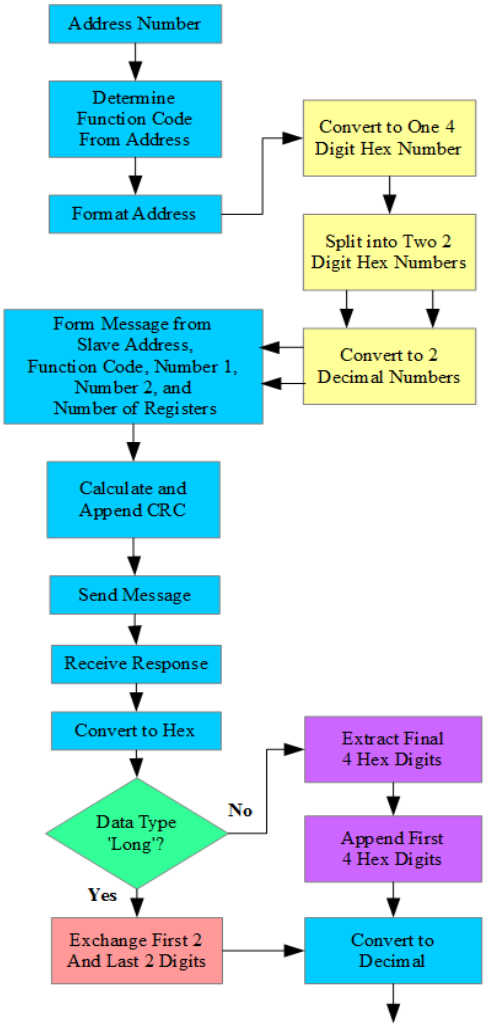

Figure 3.18: Flow chart for Modbus protocol

Communication to the FPGA is done through built-in MATLAB commands using User Datagram Protocol (UDP). With the IP address of the FPGA, MATLAB can ping the FPGA and receive all the data stored on the board. This type of communication happens quickly, and allows for faster control using the transferred data.

The load bank is controlled by a separate computer than the one controlling the CES unit, primarily to reduce the amount of applications running on the CES control

computer. The two computers are connected through TCP/IP protocol, but share only access to critical files with each other. Communication to the load bank is done through a serial cable and two software packages provided by NHR. One software package allows for manual operation of the load bank, while the other accepts comma separated values to build a load profile which runs in real time automatically.

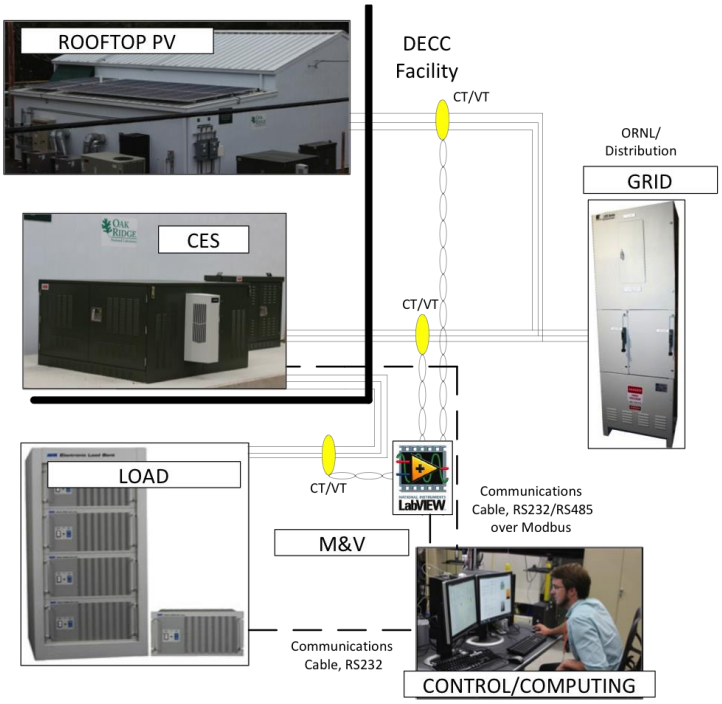

Figure 3.19: Communication channels to all hardware

3.3.4. Safety

For some of the applications being tested, the CES is required to operate for 24 hours a day. In order to keep track of the system, standalone programs were developed in MATLAB to monitor the unit and report errors to the users. If there were ever an error that occurred during operation, the CES monitoring program would stop the operation of

the unit and send text messages to ORNL employee cell phones and email notifications to team members with details about the error that occurred. Then, a team member could remotely log in to the computer controlling the unit to verify that the unit had stopped and do analysis on what caused the error.

There is also a standalone MATLAB program which was developed to monitor the temperature in the room containing the load bank. The load bank room has a thermocouple on the fire detector on the ceiling, on the outlet of the load bank, and on the inlet of the air conditioning unit. The thermocouples interface to the CES control computer through a serial connection and are constantly monitored by the thermal management program. The thermocouples have individual temperature thresholds which, when violated, cause the CES GUI to shut down both the CES unit and the load bank immediately to mitigate the risk of fire. In the event of shutdown, the CES monitoring program would also send text and email alerts to team members.

CHAPTER IV
RESULTS

4.1. Load Factor

To perform a real test on load factor control, a load profile is generated using the RST with the occupant models described in Table A.1. An example result from the RST is shown in Figure 4.1. The peak load for this profile is 16.037 kW and the average load for this profile is 3.147 kW, making the load factor before control 0.1963. Next, the set points are optimized to bring the load factor closer to unity.

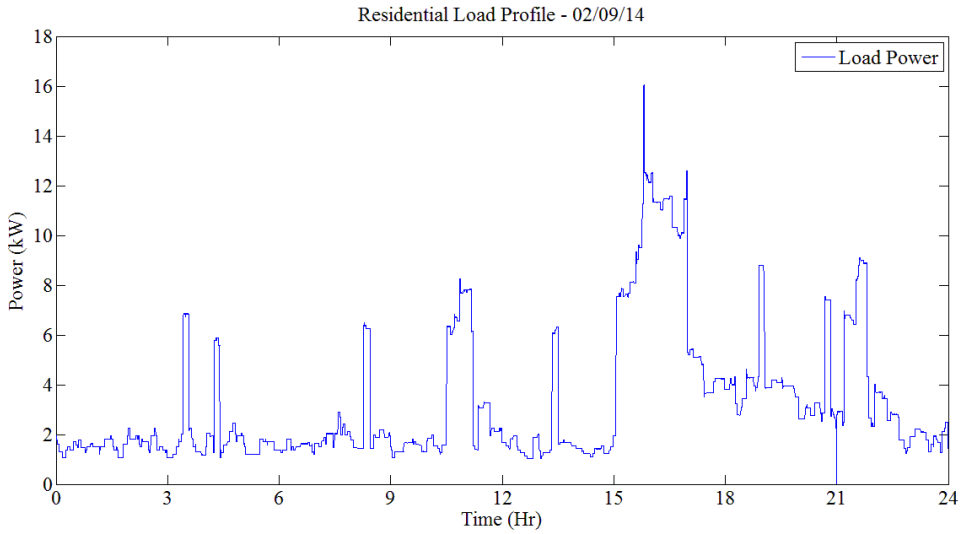

Figure 4.1: Residential simulation tool result

To determine the optimum placement of the set points, the load profile is passed to the GA program with the battery model and fitness function. Once the GA program completes, it returns the two optimum set points, the SOC estimate for the day, and the new load factor after control. For the profile in Figure 4.1, GA returned 5.405 kW as the

high set point and 3.463 kW as the low set point, making the new load factor 0.7148. The original residential profile, new residential profile, set points, and SOC estimate are all shown in Figure 4.2. All of these parameters are passed to the control GUI for 24 hour testing.

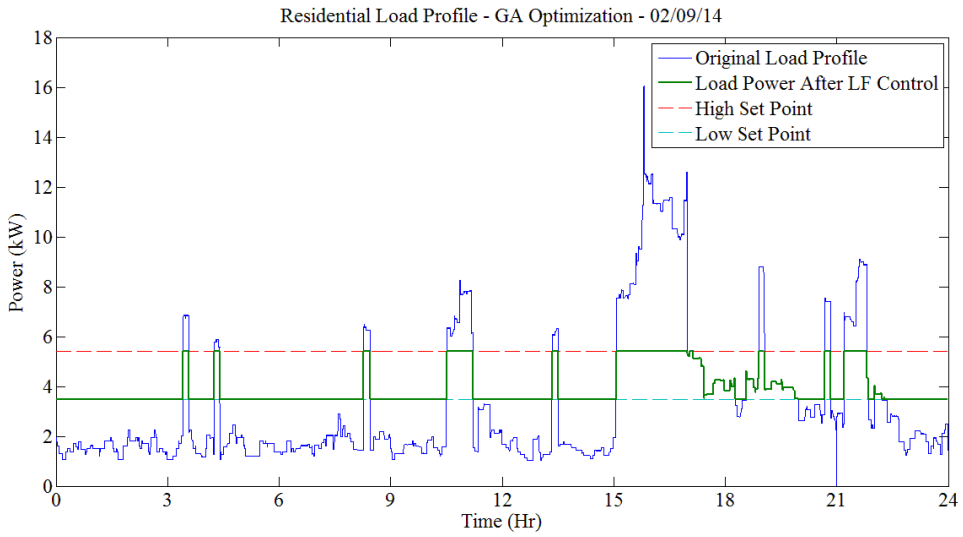

Figure 4.2: Genetic algorithm simulation result

With all the parameters described above, all the necessary data for a real world test is ready. The load profile is programmed into the load bank. The set points and SOC estimate are loaded into the control GUI. The control scheme for load factor control was activated and run for 24 hours. The results of the test are shown in Figure 4.3.

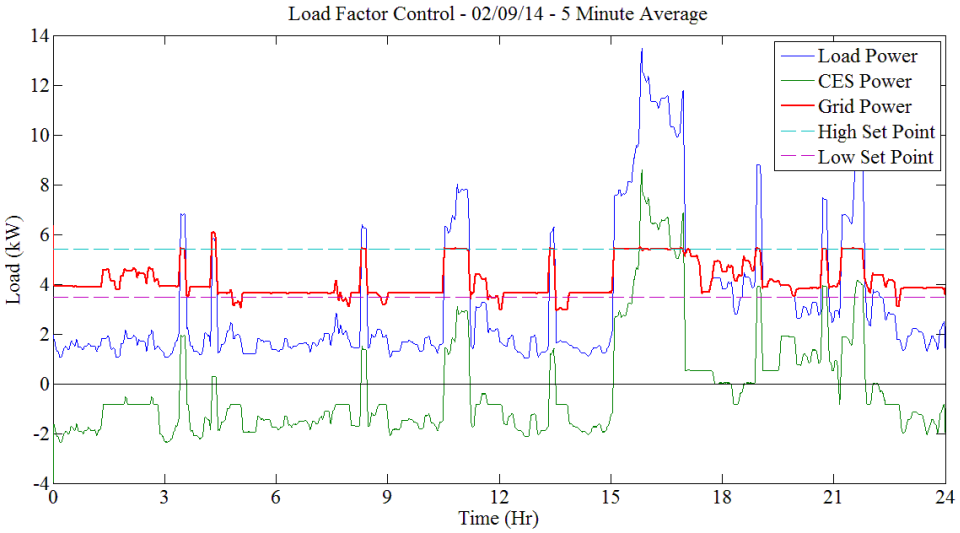

Figure 4.3: Load factor test result with 5 minute average

From the results of Figure 4.4, the calculated load factor seen by the grid is 0.6469. This is a significant increase over the original load factor of 0.1963, but not quite as large of an increase compared to the simulation load factor of 0.7148. Note also that the peak load seen by the grid was reduced by over 50%. Figure 4.4 shows the error between the predicted grid power and the actual grid power.

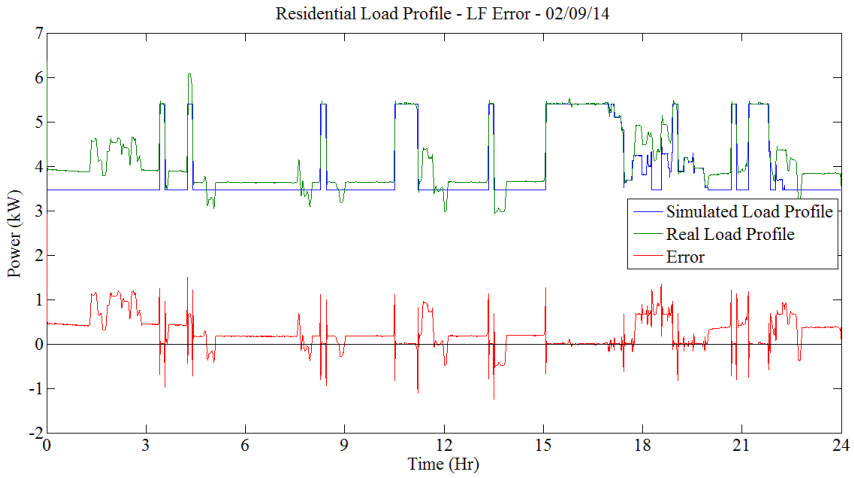

Figure 4.4: Load factor error

Figure 4.4 shows that at some points during the testing, the grid power went outside of the set points. This normally occurs when the grid power is outside of the set point by a value less than the control dead band power. There is a minimum power the inverter can provide or absorb, and if a power is requested under the minimum, then no power transfer occurs. The minimum power can be adjusted; however as the minimum gets closer to zero, more current harmonics are injected into the system.

Another portion of the error occurs when the simulation assumed that the grid power would be at the low set point, but during the test the grid power stayed slightly above the set point. This is an intentional design characteristic of the load factor controller. If the SOC of the CES is not the same as the predicted SOC returned from GA, then the controller will attempt to compensate by absorbing or discharging slightly more power, as long as the extra power does not push the grid power outside of the set points. Figure 4.5 shows how the SOC changes over the course of the day.

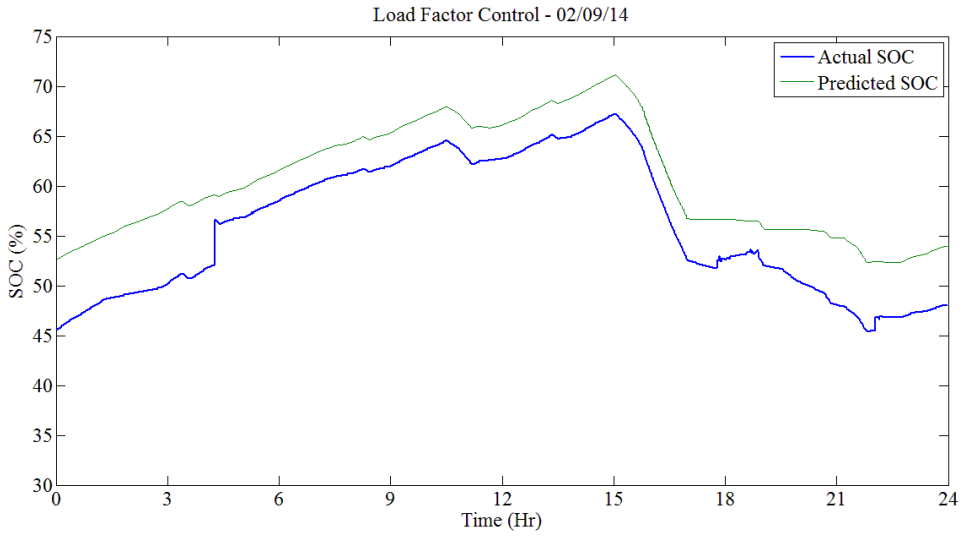

Figure 4.5: SOC during load factor test

The actual SOC curve in Figure 4.5 represents the SOC measurement being received from the CES unit. The predicted SOC curve shows how the battery model and GA optimization predict the SOC will behave. The prediction expects the starting SOC of the unit to be 53%, when in reality the starting SOC was 46%. The SOC prediction uses the ending SOC from the previous day's simulation as the starting SOC for the next day. In this case, the SOC was predicted to be higher at the end of the previous day than it actually ended up being, hence the SOC prediction is higher than the measurement at the start of the day. Except for the initial offset, the measurement and prediction curves are quite similar in shape. Because the curves are similarly shaped, the error is fairly constant throughout the 24 hours of the test and never reaches a difference of more than 7.5%. This can be seen in Figure 4.6, which shows the error between the predicted SOC and the measured SOC. The error curve has a small positive slope, so the error is mostly constant but slightly increasing. This error can be attributed to the efficiency and auxiliary load assumptions in the battery model. The error is also affected by the determination of the SOC by the BMS, which is based on a number of parameters not accessible through the MODBUS communication to the unit.

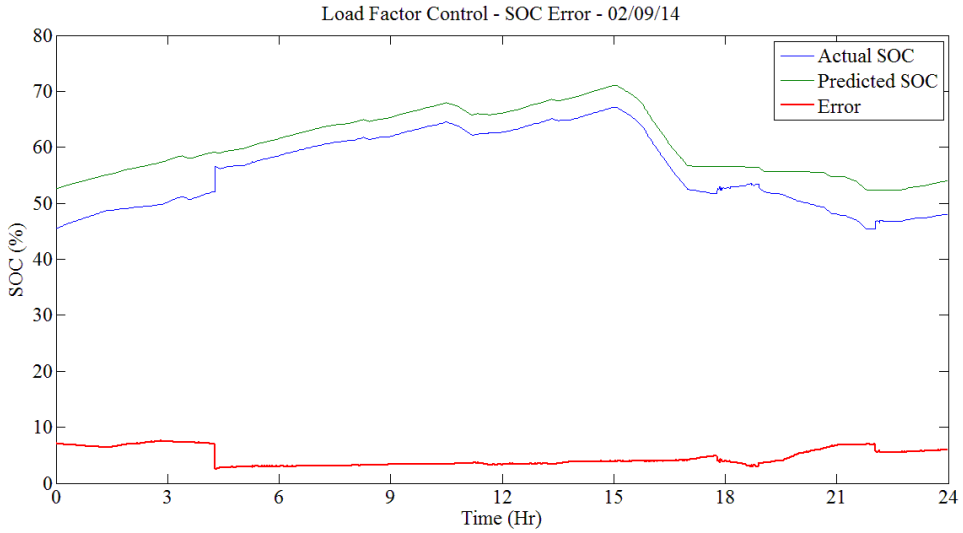

Figure 4.6: SOC error during load factor test

More results from load factor testing can be found in Figures A.4 – A.14.

4.2. PV Smoothing

For the PV smoothing application, the cloud cover and temperature data are collected and stored to be used by the neural network to predict the irradiance and power output of the PV array. With the temperature and cloud cover data collected, if the NN is trained, then an irradiance and PV power prediction can be made. The NN creates an irradiance profile, which is then fed into the PV model with the temperature data to determine the output power. The results can be seen in Figures 4.7 and 4.8. In Figure 4.8, it can be seen that the output power will begin significant ramping starting at hour 8 (8:00 am) before peaking at 6 kW at hour 14 (2:00 pm) and then dropping off to 0 by hour 20 (8:00 pm).

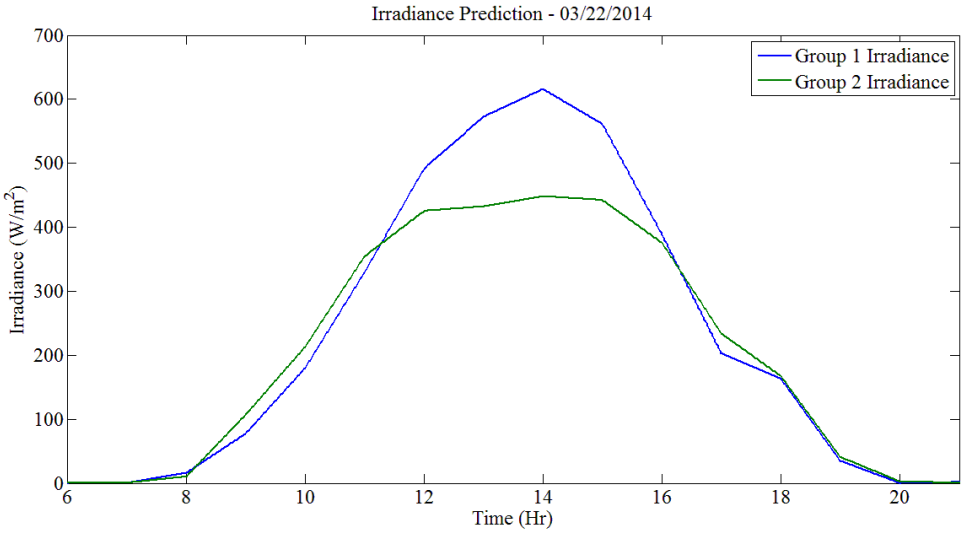

Figure 4.7: Irradiance prediction

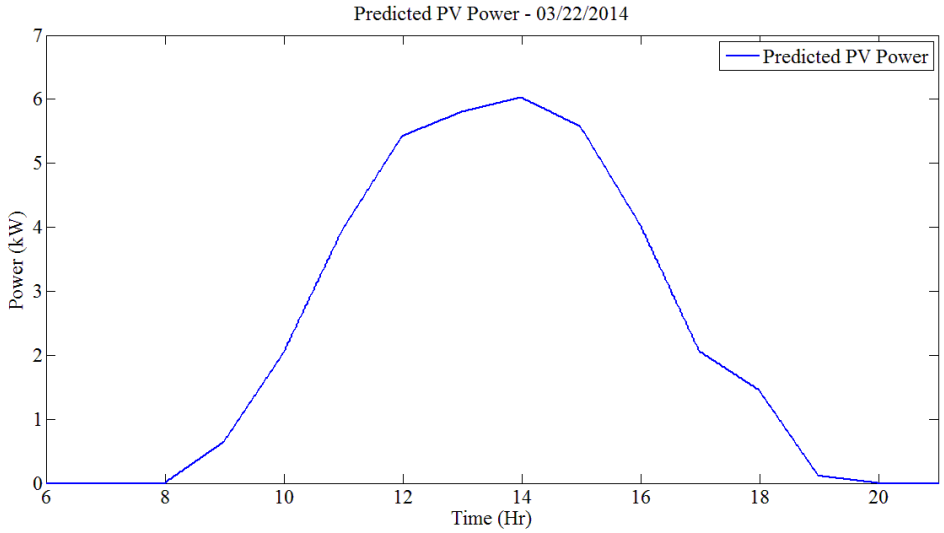

Figure 4.8: PV power prediction

With the PV output prediction, PV smoothing can be performed using the CES unit. Figure 4.9 shows the results of the smoothing.

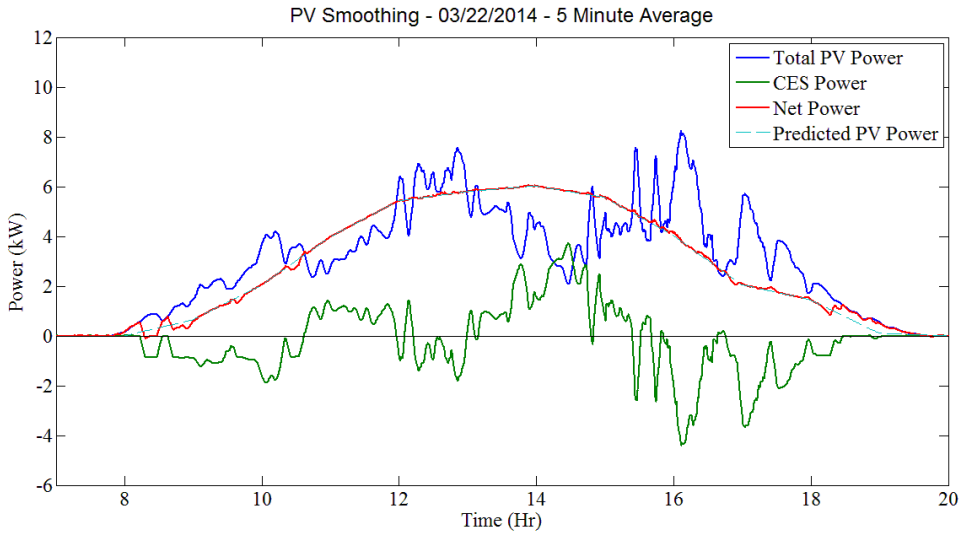

Figure 4.9: PV smoothing test results

The figure above shows that the output power of the PV array oscillated above and below the prediction. To compensate, the CES unit alternated from charging to discharging to smooth the output power. This kept the output power at or near the prediction all day. The CES unit also removed the fluctuations in power from the array. These fluctuations occurred all day for this test, with the largest event occurring at 15:27 (3:27 pm). The PV output power drops from 8.5 kW to 3.7 kW, or 35% of rated power, in 12 minutes. In the next 5 minutes, the output power increases back to 7.4 kW, a change of 27% of rated power. This fluctuation is unseen by the grid because the CES compensates by providing the lost power. Although there is a small amount of error between the prediction and the power seen by the grid, it is far less noticeable than the large power fluctuations from an unsmoothed PV array. The error can be seen in Figure 4.10.

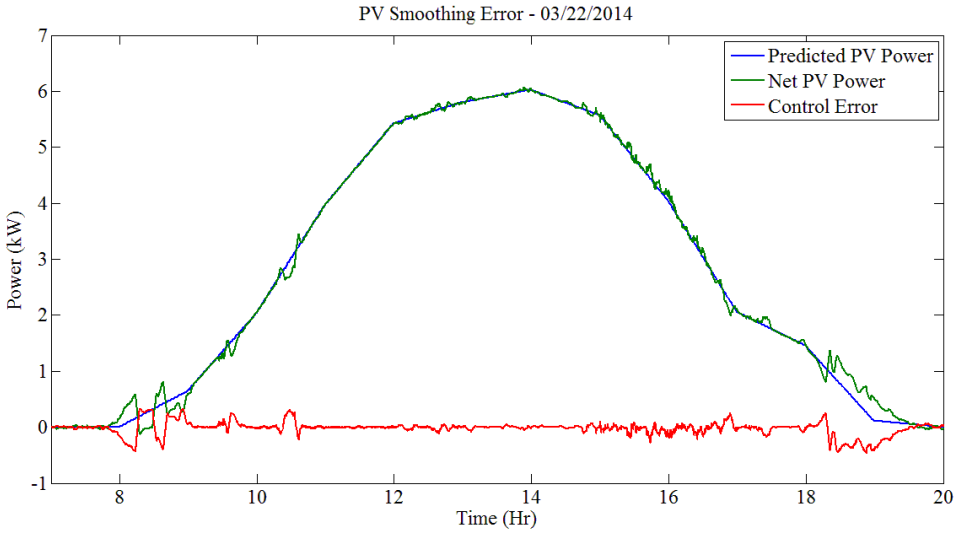

Figure 4.10: PV smoothing error

Some small fluctuations in error occur during various points in the day, mostly in the early morning and late evening. These fluctuations occur when the amount of power requested from the CES unit is within the dead band for control. This same phenomenon is seen in the load factor control results, and is explained there.

The effect of PV smoothing on SOC can be seen in Figure 4.11. Since the PV estimate was close, the CES unit charged and discharged roughly the same amount of energy over the day. This causes the SOC to stay fairly constant, rising from an original SOC of 62.5% to 64.8%. If the PV predictions continue this trend of nearly identical starting and ending SOC, then the unit will be able to run for many days on end with no SOC limit violations.

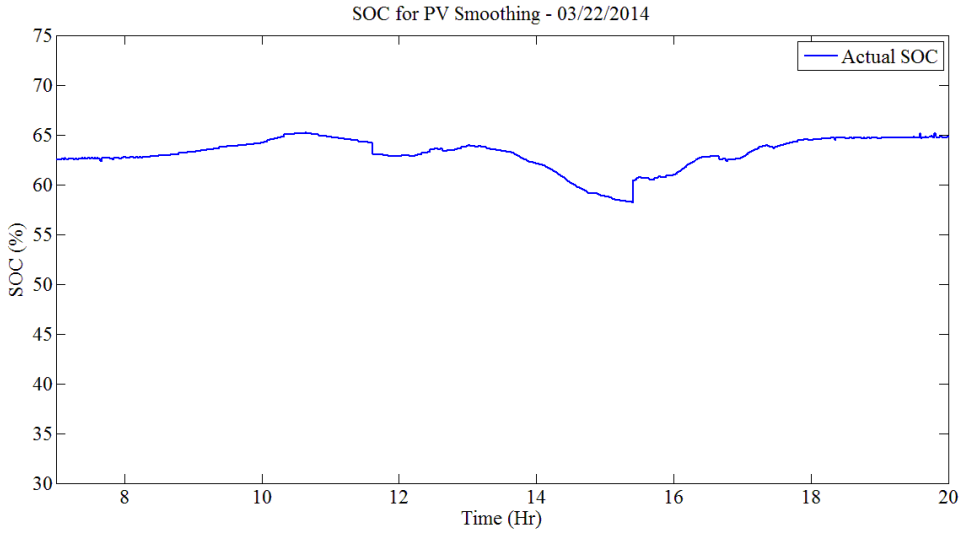

Figure 4.11: PV smoothing effect on state of charge

More results from PV smoothing can be seen in Figures A.15 – A.19.

4.3. Regulation Services

The regulation services test was performed using the test regulation signals from PJM. Since the CES unit is able to respond almost instantly to power requests, the fast regulation signal was used. Once the regulation signal had been formatted according to the testing procedure, the regulation control on the CES unit was activated and the results can be seen in Figure 4.12.

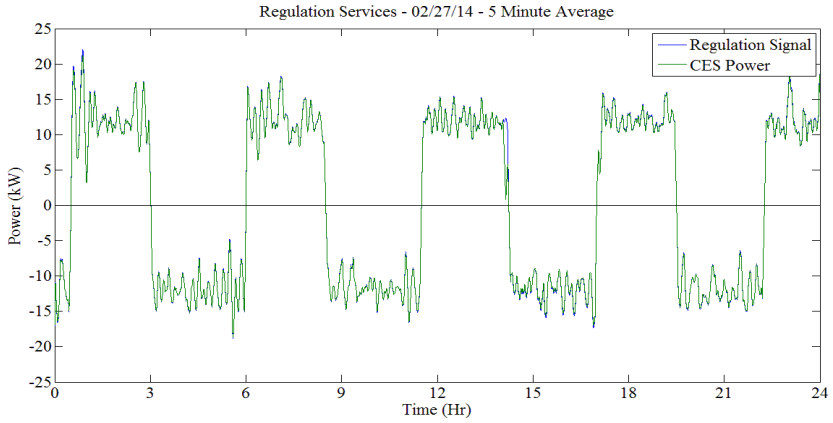

Figure 4.12: Regulation test results

The above figure shows how the CES unit responded to the fast regulation signal. The unit is able to provide all the power requested from the signal for a little less than three hours. At that point, the CES must change its charge/discharge state to balance the SOC. This transition occurs only when the unit's SOC reaches a high or low limit. The cycling of the SOC can be seen in Figure 4.13. During the 24 hour test, the battery completely cycles within its limits 4 times. Comparing this to Figure 4.5 and Figure 4.11, it can be seen that providing regulation in this way has the largest number of cycles per day. Aggregation of many storage systems should help eliminate the need to operate in such a way.

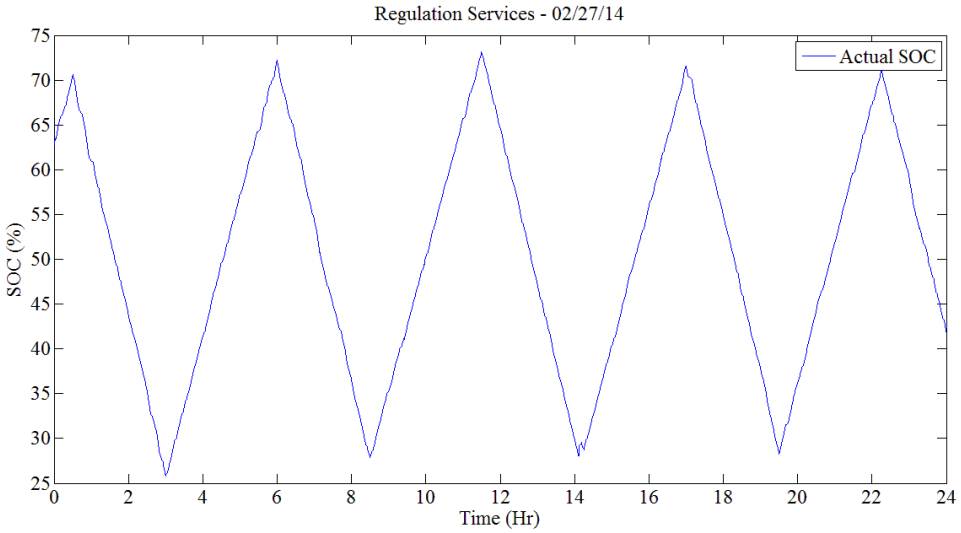

Figure 4.13: Regulation effect on state of charge

More results from provision of regulation services can be seen in Figures A.20 – A.24.

CHAPTER V
CONCLUSIONS AND FUTURE WORK

5.1. Conclusion

The benefits from using ESS for grid applications support the continued research into low cost energy storage. With increased uncertainty on the generation side, energy storage provides stability and flexibility to a renewable-rich grid. Many forms of energy storage exist, but this thesis focuses on the utilization of secondary-use electric vehicle batteries for community energy storage. The opportunities for CES units like these are numerous. By employing electric vehicle batteries which no longer fulfill their primary role, both the utility and the battery manufacturer benefit. Purchasing used batteries relieves some of the capital cost of energy storage for the utility, and the battery manufacturer can sell the same battery twice. Also, the manufacturer can avoid or at least defer the cost of dismantling the batteries by recycling them as CES units.

To be worth creating, CES units must be able to provide more value than they cost. CES units provide value by performing grid applications which benefit the owner of the units. One potential application is PV smoothing. By using a CES unit to suppress output power fluctuations from a PV array, the power seen by the grid will be very predictable. To show this, a PV power prediction program was developed to take in temperature and cloud cover forecasts for the day and return the output power of the PV array on a one hour time scale. The program does this using neural network (NN), which makes predictions for highly nonlinear systems based off of previously collected input and output data. Once the PV output power was predicted, the prediction was given to the control GUI to perform a real world test. It was shown that the CES made the net output

power much more predictable by removing the output power fluctuations from the PV array.

Another application investigated was load factor control. The load factor of a customer is determined by dividing the average load by the peak load for a given time period. A load factor of unity represents a load which is completely constant, which also means it is fully predictable. To test how well the CES unit can control the load factor, a simulated residential load profile for three homes was obtained using the RST [36]. Then, set points for the CES unit were determined by feeding the residential load profile and battery model into GA. GA searches for an optimum based on a fitness function which prioritizes load factor, SOC, and end-of-day energy. By optimizing the location of the set points, it is possible to get the most usage out of the CES unit. Once the set points were returned by GA, they were given to the control GUI for the real testing. The residential load profile was programmed into the load bank, and the load factor application activated in the GUI. The grid saw a significant increase in load factor, and a reduced peak load, as verified in the field test.

Tests on the potential for CES units to provide regulation services were also presented. Regulation services account for small variations in the load and are essential to maintaining system stability. One CES unit will not be able to provide a large amount of regulation, but multiple units could provide a significant regulation when aggregated. Regulation was tested using historical regulation signals obtained from PJM. The signals were given a bias and loaded into the control GUI. The bias and control scheme assures that the CES unit can always provide regulation regardless of the SOC. With this method,

it was shown that the CES unit could provide regulation to the grid effectively, at the expense of a high number of battery cycles.

5.2.Future Work

5.2.1. Economic Optimization

With the data presented in this thesis, it is apparent that secondary-use CES units are capable of performing many different and valuable grid applications. The next step is to determine the value of those applications, and which ones provide the largest revenue stream for the utility. This problem is non-trivial, as different grid scenarios warrant different CES applications. Using economic optimization, it is possible to determine the scenarios and penetration levels which make CES units profitable. For example, regulation may only be profitable with 100 CES units. Any less, and the benefit does not exceed the cost of the units. Economic optimization is also heavily dependent on the lifetime of a CES unit. Certain applications may cause the CES to become unusable after 3 years, but other applications may allow the CES to operate for 8 or more years. Determining the value and lifetime for different scenarios will give an insightful look into how CES units can best be utilized.

5.2.2. Commercial / Industrial Applications Analysis

This thesis explores the use of secondary-use CES units at a residential scale. Another possible use of secondary-use batteries would be on the commercial or industrial scale. Typically, commercial and industrial customers would have a larger total load than a residential customer. This would most likely require a larger amount of energy storage

to effectively perform applications. Larger units for secondary-use batteries are possible, and could provide substantial support for commercial and industrial customers. For example, many commercial and residential customers pay a demand charge for their peak load throughout the year. This charge can be many times more expensive than the normal electric rate, and can represent a large portion of the customer's total energy bill. By using secondary-use battery units to provide the peak load, the demand charge can be lowered. This is only one of many possible applications for commercial and industrial customers. Additional research in this area would provide insight into how to best harness the potential of secondary-use electric vehicle batteries for use in the electric grid.

LIST OF REFERENCES

[1] A. Akhil et al. "DOE/EPRI 2013 Electricity Storage Handbook in Collaboration with NRECA," Sandia National Laboratories, Albuquerque, New Mexico and Livermore, California, 2013.

[2] *DOE Global Energy Storage Database* [Online]. Available: http://www.energystorageexchange.org/projects

[3] *Raccoon Mountain Pumped-Storage Plant* [Online]. Available: http://www.tva.gov/sites/raccoonmt.htm

[4] "Updated Capital Cost Estimates for Utility Scale Electricity Generating Plants," U.S. Energy Information Administration, April 2013.

[5] Narula, C., et al. "Economic Analysis of Deploying Used Batteries in Power Systems," Oak Ridge National Laboratory, June 2011.

[6] *What the duck curve tells us about managing a green grid* [Online]. Available: http://www.caiso.com/Documents/FlexibleResourcesHelpRenewables_FastFacts.pdf

[7] Malinowski, J. and K. Kaderly, "Peak shaving - a method to reduce utility costs," Region 5 Conference: Annual Technical and Leadership Workshop, 2004.

[8] *About Li-ion Batteries* [Online]. Available: http://www.nexeon.co.uk/technology/about-li-ion-batteries/

[9] Barnes, A. K., et al. "Optimal battery chemistry, capacity selection, charge/discharge schedule, and lifetime of energy storage under time-of-use pricing," 2nd IEEE PES International Conference and Exhibition on Innovative Smart Grid Technologies (ISGT Europe), 2011.

[10] "EPRI-DOE Handbook of Energy Storage for Transmission &Distribution Applications," EPRI, Palo Alto, CA, and the U.S. Department of Energy, Washington, DC: 2003. 1001834.

[11] *Energy Storage: Packing Some Power* [Online]. Available: http://www.economist.com/node/21548495?frsc=dg|a

[12] S. Faias et al. "An Overview on Short and Long-Term Response Energy Storage Devices for Power Systems Applications," Technical University of Lisbon, IST/TUL, Portugal, 2007.

[13] A. Gebremedhin et al. "Seasonal Heat Storages in District Heating Systems," Linköping University, Linköping, Sweden.

[14] S. Lemofouet et al, "A hybrid energy storage system based on compressed air and supercapacitors with maximum efficiency point tracking (MEPT)," *IEEE Transactions on Industrial Electronics*, vol. 53, no. 4, August 2006.

[15] R. Hebner et al, "Flywheel batteries come around again," *IEEE Spectrum*, vol. 39, no. 4, pp. 46-51, April 2002.

[16] Onar, O. C., et al. "Modeling, controls, and applications of community energy storage systems with used EV/PHEV batteries," IEEE Transportation Electrification Conference and Expo (ITEC), 2012.

[17] Broussely, M., et al. "Main aging mechanisms in Li ion batteries." *Journal of Power Sources* 146(1–2): 90-96, 2005

[18] Broussely, M., et al. "Lithium ion: the next generation of long life batteries characteristics, life predictions, and integration into telecommunication systems,"

Twenty-second International Telecommunications Energy Conference (INTELEC), 2000.

[19] Marano, V., et al. “Lithium-ion batteries life estimation for plug-in hybrid electric vehicles,” IEEE Vehicle Power and Propulsion Conference (VPPC), 2009.

[20] Sarre, G., et al. "Aging of lithium-ion batteries." *Journal of Power Sources* 127(1–2): 65-71, 2004.

[21] Shim, J., et al. "Electrochemical analysis for cycle performance and capacity fading of a lithium-ion battery cycled at elevated temperature." *Journal of Power Sources* 112(1): 222-230, 2002.

[22] Zhang, Y. and Wang, C., “Cycle-Life Characterization of Automotive Lithium-Ion Batteries with $LiNiO_2$ Cathode,” The Pennsylvania State University, May 8, 2009.

[23] Kalhammer, F., et al. “Status and Prospects for Zero Emissions Vehicle Technology,” ARB Independent Expert Panel, 2007.

[24] *GM Envisions Refreshing EV Batteries* [Online]. Available: http://news.cnet.com/8301-11128_3-20022049-54.html

[25] *Electric generator dispatch depends on system demand and the relative cost of operation* [Online]. Available: http://www.eia.gov/todayinenergy/detail.cfm?id=7590

[26] *View Generic Load Profiles* [Online]. Available: https://www.comed.com/customer-service/rates-pricing/retail-electricity-metering/Pages/res-generic-profiles.aspx

[27] *Electric Rates Schedules* [Online]. Available: https://www.kub.org/wps/portal/Customers/Home/BusinessCustomers/BusinessRates/ElectricRates

[28] Eftekharnejad, S., et al. "Impact of increased penetration of photovoltaic generation on power systems." *IEEE Transactions on Power Systems*, 28(2): 893-901, 2013.

[29] Shao, M., et al. "Steady-state methodology for investigating the relationship between photovoltaic (PV) facility size, location, and voltage impact," IEEE Power and Energy Society General Meeting, 2012.

[30] Junseok, S., et al. "Development of a Markov-Chain-Based Energy Storage Model for Power Supply Availability Assessment of Photovoltaic Generation Plants." *IEEE Transactions on Sustainable Energy* 4(2): 491-500, 2013.

[31] Alquthami, T., et al. "Study of photovoltaic integration impact on system stability using custom model of PV arrays integrated with PSS/E." North American Power Symposium (NAPS), 2010.

[32] Tsang, K. M., et al. "Lithium-ion battery models for computer simulation," IEEE International Conference on Automation and Logistics (ICAL), 2010.

[33] Speltino, C., et al. "Comparison of reduced order lithium-ion battery models for control applications," Proceedings of the 48th IEEE Conference on Decision and Control, held jointly with the 28th Chinese Control Conference (CDC/CCC), 2009.

[34] Lijun, G., et al. "Dynamic lithium-ion battery model for system simulation." *IEEE Transactions on Components and Packaging Technologies*, 25(3): 495-505, 2002.

[35] Erdinc, O., et al. “A dynamic lithium-ion battery model considering the effects of temperature and capacity fading,” International Conference on Clean Electrical Power, 2009.

[36] Chen, S. X., et al. “Modeling of Lithium-Ion Battery for Energy Storage System Simulation,” Asia-Pacific Power and Energy Engineering Conference (APPEEC), 2009.

[37] Villalva, M. G., et al. "Comprehensive Approach to Modeling and Simulation of Photovoltaic Arrays." *IEEE Transactions on Power Electronics* 24(5): 1198-1208, 2009.

[38] Johnson, Brandon Jeffrey, "An Occupant-Based Dynamic Simulation Tool for Predicting Residential Power Demand and Quantifying the Impact of Residential Demand Response." Master's Thesis, University of Tennessee, 2013. http://trace.tennessee.edu/utk_gradthes/2613

[39] *Wunderground* [Online]. Available: http://www.wunderground.com/cgi-bin/findweather/getForecast?query=zmw:37830.1.99999

[40] *Clouds Forecast for Astronomical Purposes* [Online]. Available: http://weather.gc.ca/astro/clds_vis_e.html

[41] Guyer, J. P., “Introduction to Electrical Power Requirements for Buildings,” Continuing Education and Development, Inc., Stony Point, NY, 2010.

[42] *Fast Response Regulation Signal* [Online]. Available: http://www.pjm.com/markets-and-operations/ancillary-services/mkt-based-regulation/fast-response-regulation-signal.aspx

APPENDIX

Table A.1: Occupants and loads for residential simulation

Load	*Home 1*	*Home 2*	*Home 3*
Number of Occupants	4	3	5
Heat Pump	No	Yes	No
Nonelectric Heating	Yes	No	Yes
Air Conditioning	Yes	Yes	Yes
Water Heater	No	Yes	No
Refrigerator	Yes	Yes	Yes
Automatic Defrost	Yes	Yes	Yes
Second Refrigerator	Yes	No	No
Automatic Defrost	Yes	No	No
Freezer	Yes	Yes	No
Automatic Defrost	Yes	No	No
Washer	Yes	Yes	Yes
Electric Dryer	Yes	Yes	Yes
Dishwasher	Yes	No	Yes
Cooking	Yes	Yes	Yes
Lighting	Yes	Yes	Yes
Number of Televisions	3	3	3
Number of Computers	2	2	2

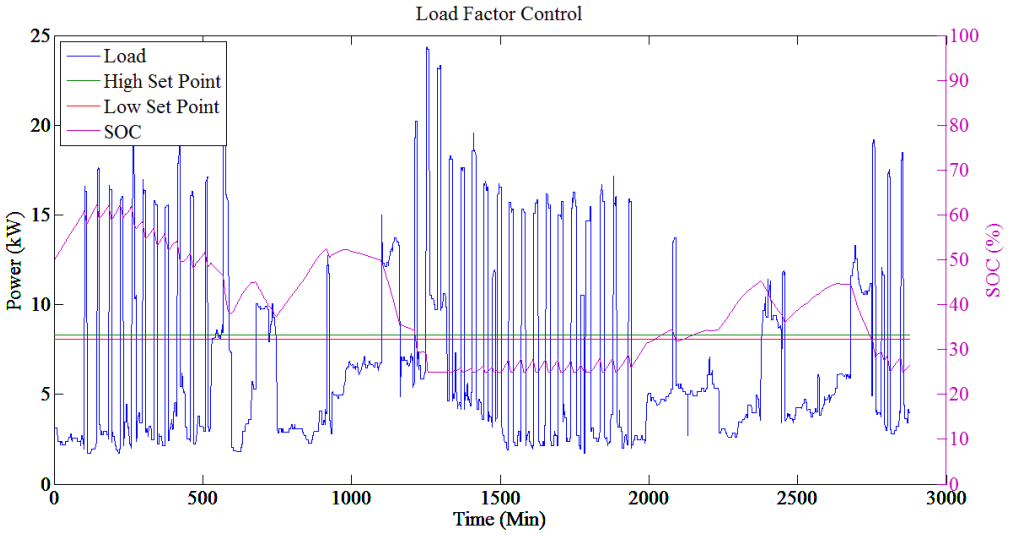

Figure A.1: Set points too low – SOC hits minimum

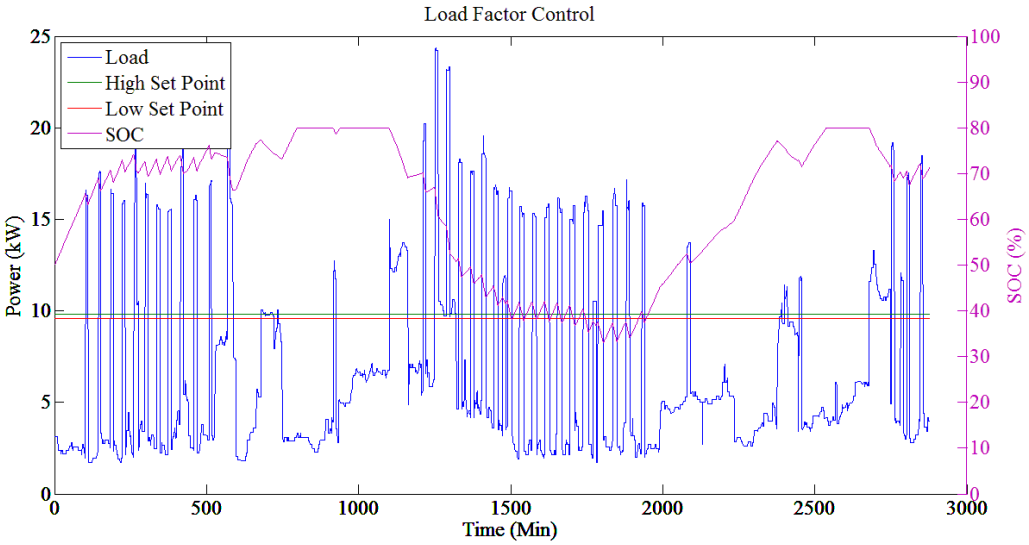

Figure A.2: Set points too high – SOC hits maximum

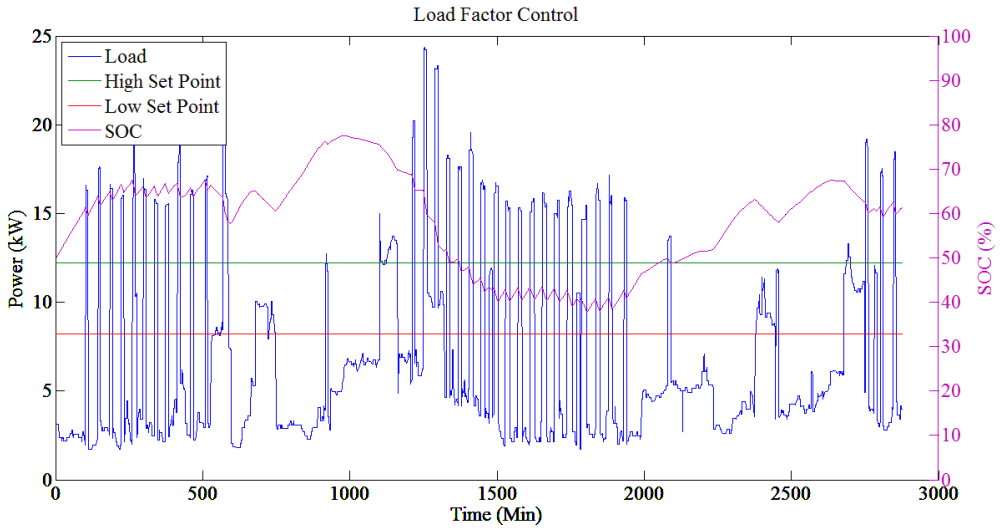

Figure A.3: Set points too far apart – non-optimal solution

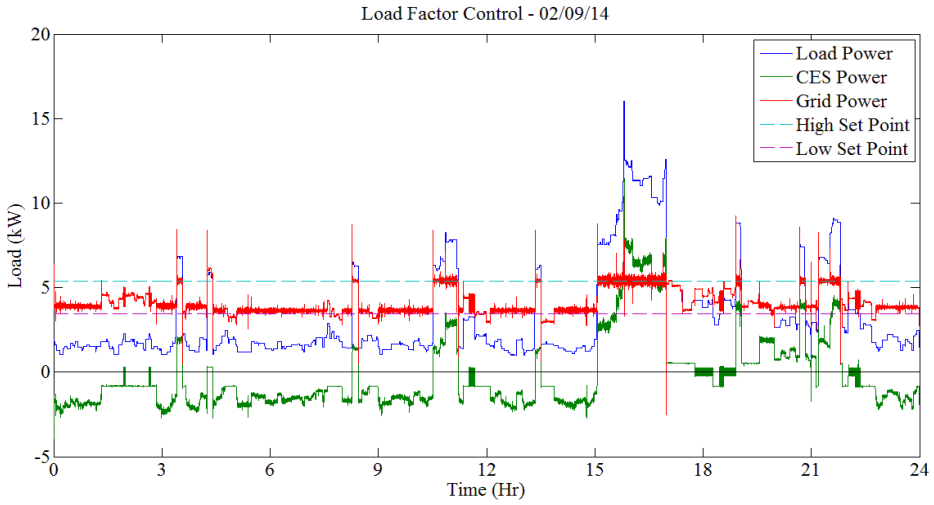

Figure A.4: Results from Figure 4.3 – no averaging

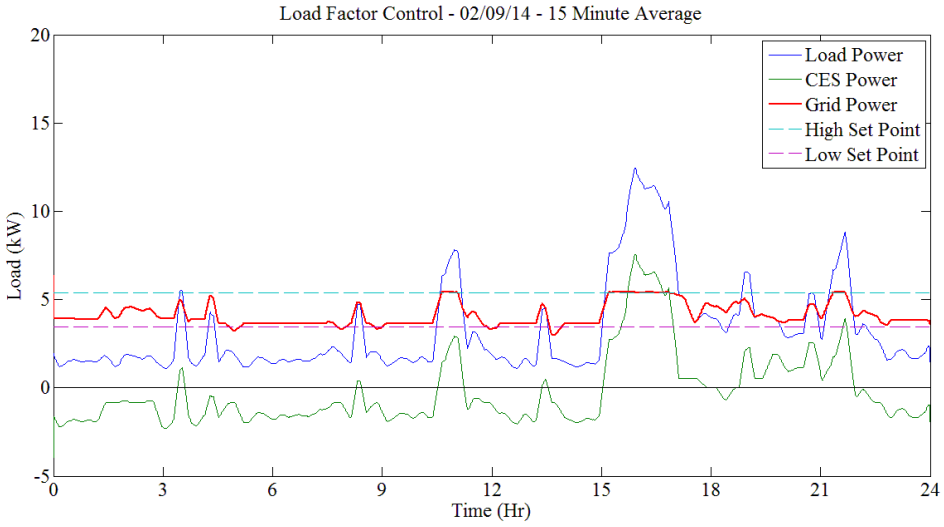

Figure A.5: Results from Figure 4.3 – 15 minute average

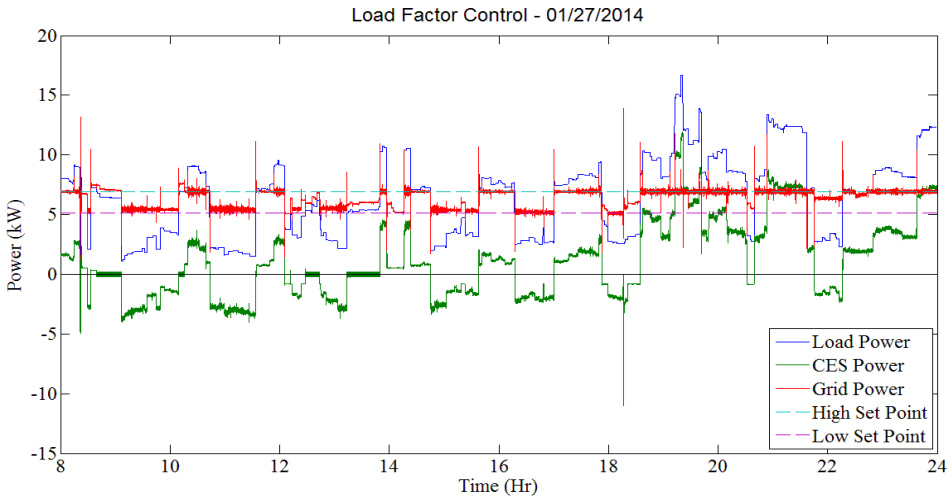

Figure A.6: Results from load factor control 01/27/2014 – no averaging

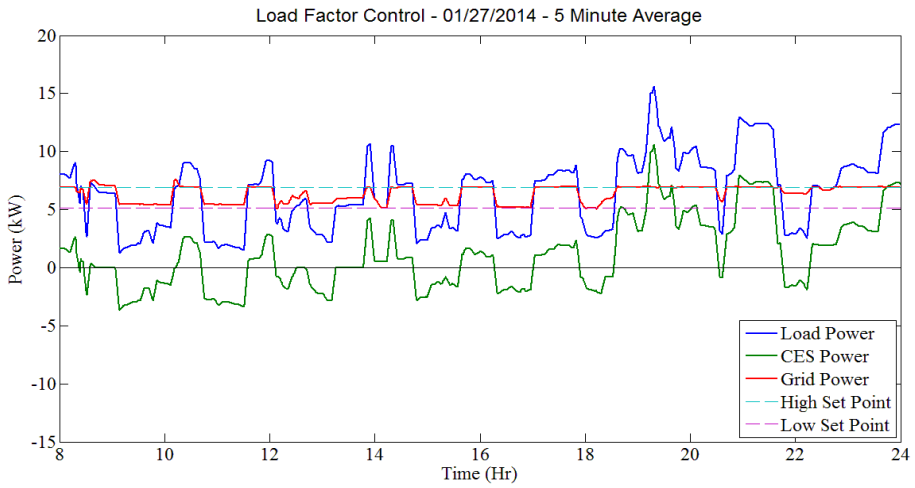

Figure A.7: Results from load factor control 01/27/2014 – 5 minute average

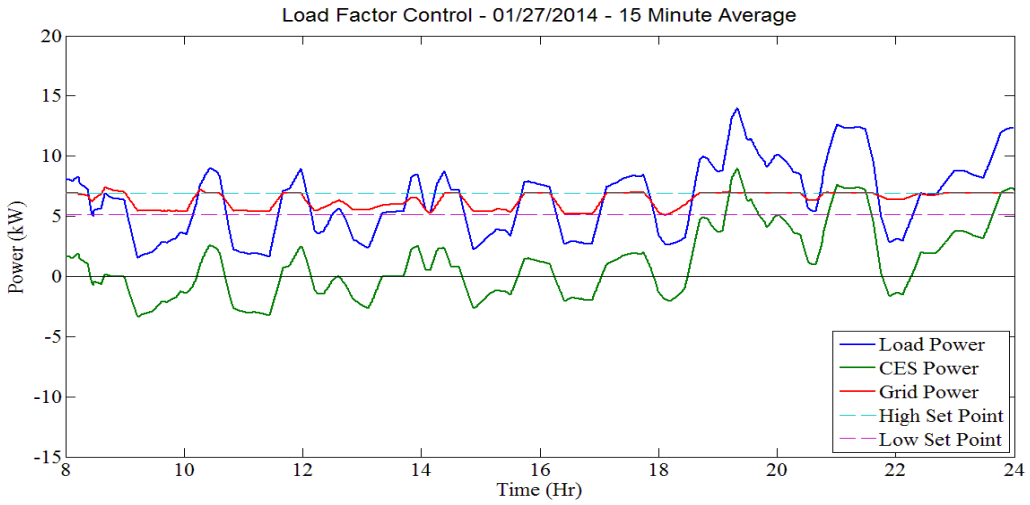

Figure A.8: Results from load factor control 01/27/2014 – 15 minute average

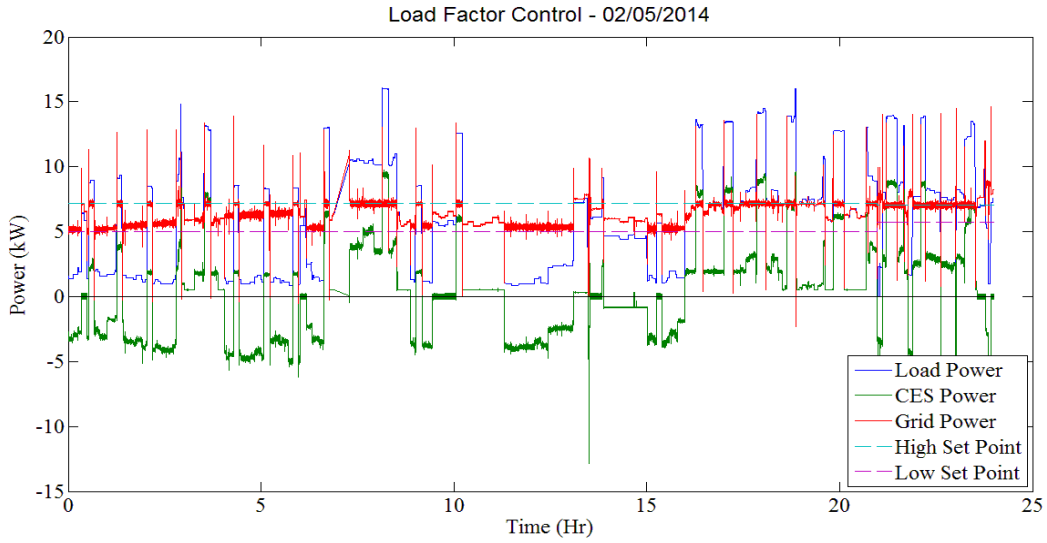

Figure A.9: Results from load factor control 02/05/2014 – no averaging

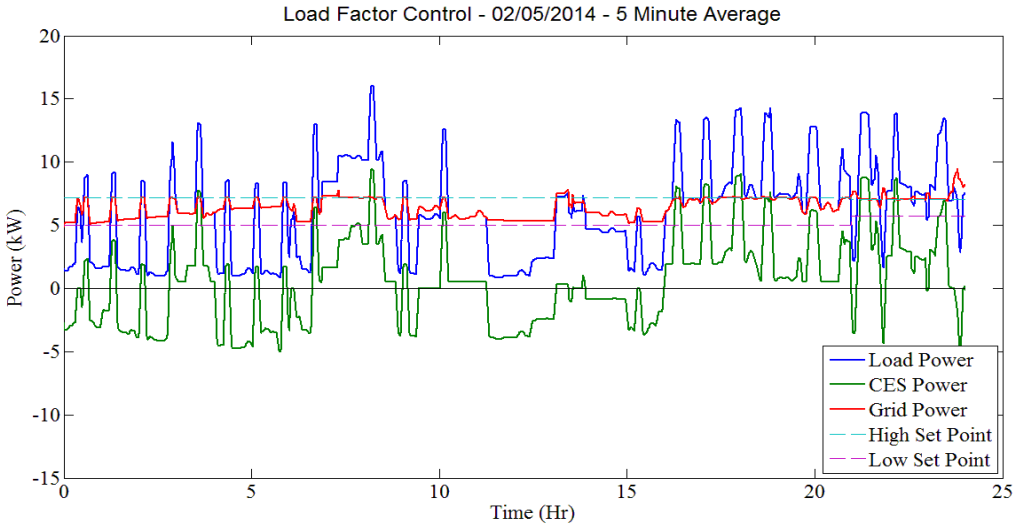

Figure A.10: Results from load factor control 02/05/2014 – 5 minute average

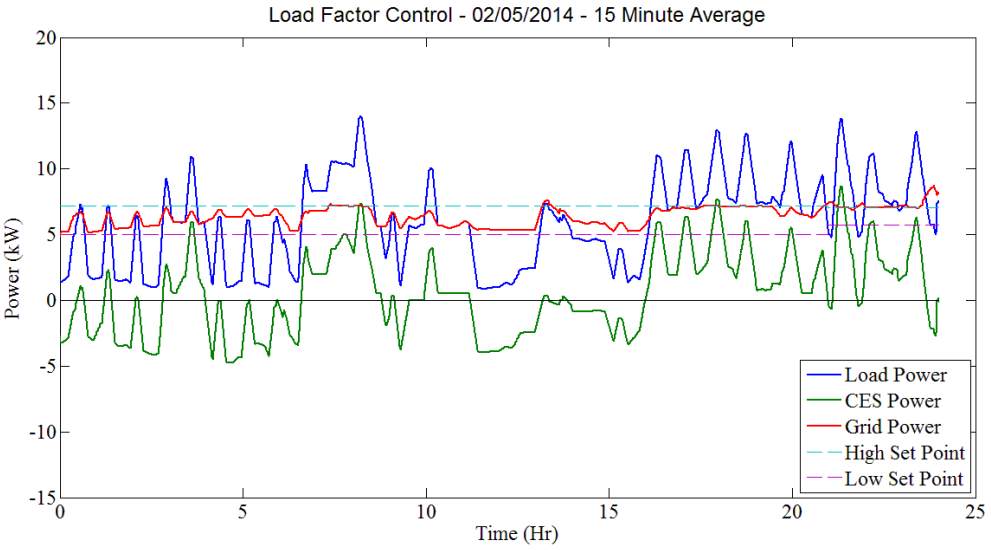

Figure A.11: Results from load factor control 02/05/2014 – 15 minute average

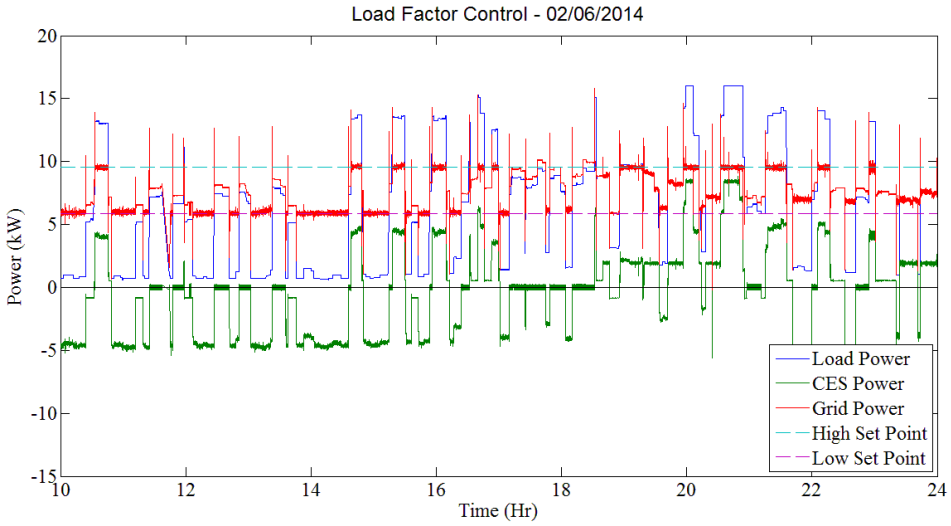

Figure A.12: Results from load factor control 02/06/2014 – no averaging

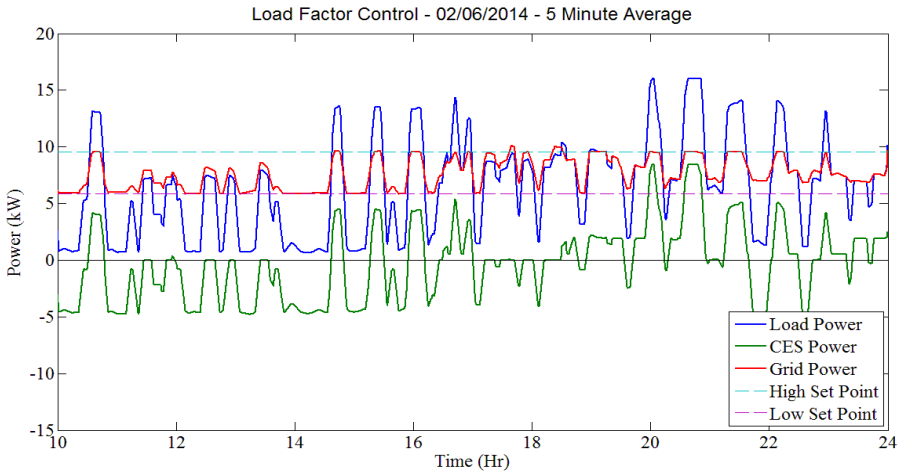

Figure A.13: Results from load factor control 02/06/2014 – 5 minute average

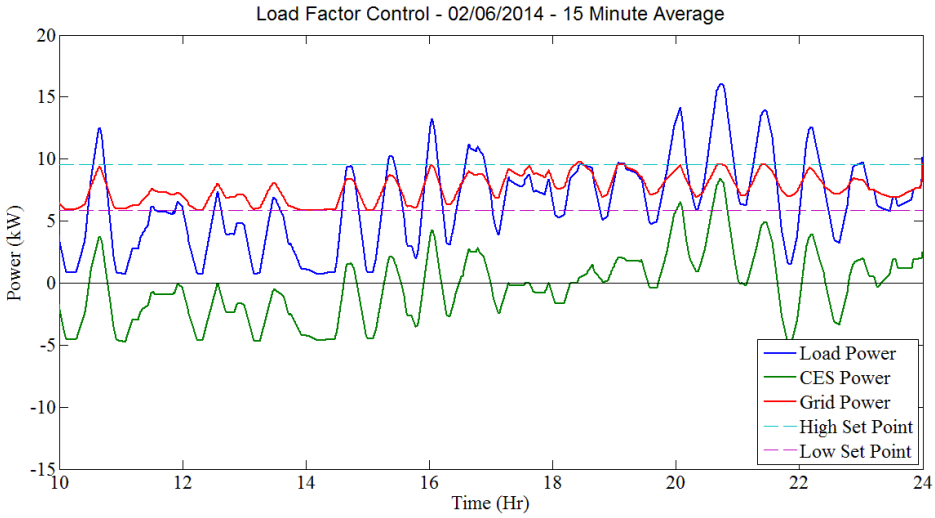

Figure A.14: Results from load factor control 02/06/2014 – 15 minute average

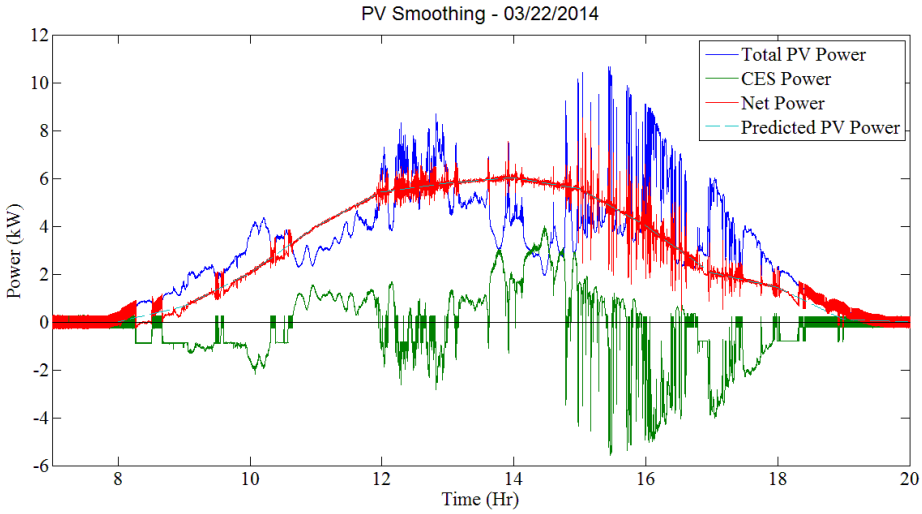

Figure A.15: Results from Figure 4.9 – no averaging

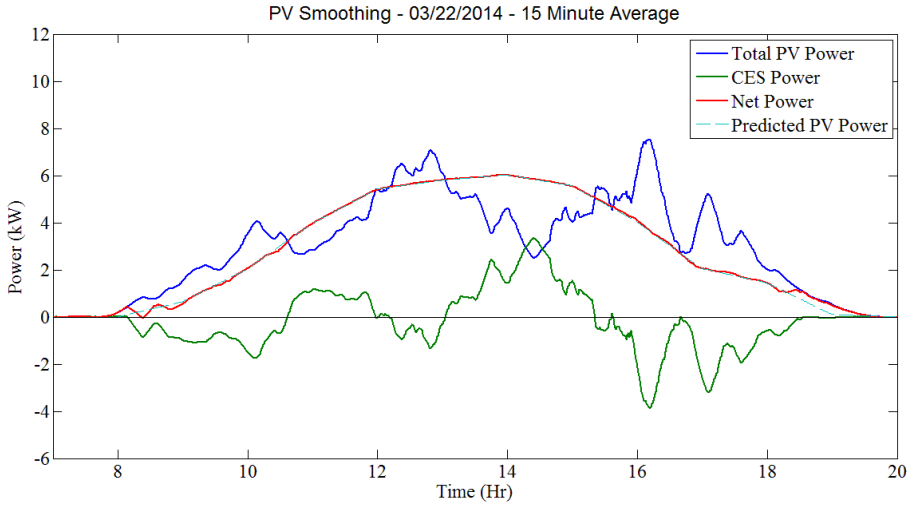

Figure A.16: Results from Figure 4.9 – 15 minute average

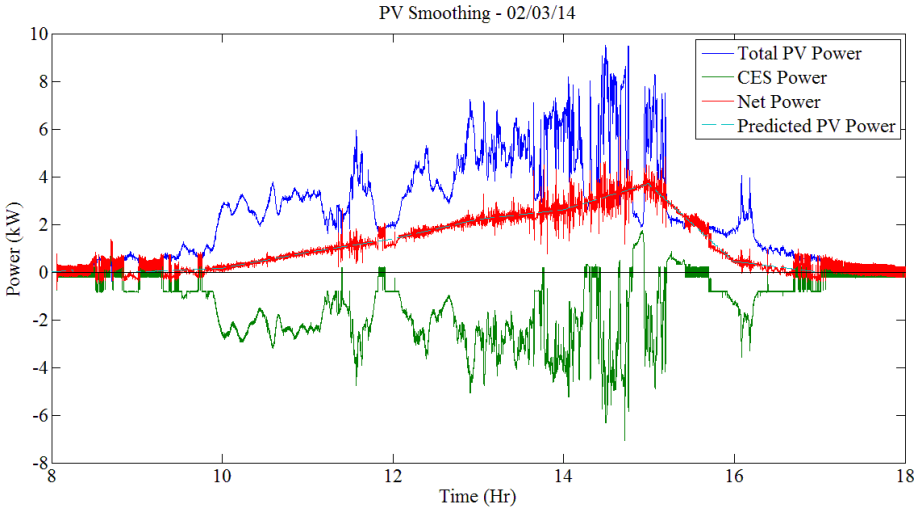

Figure A.17: Results from PV smoothing 02/03/2014 – no averaging

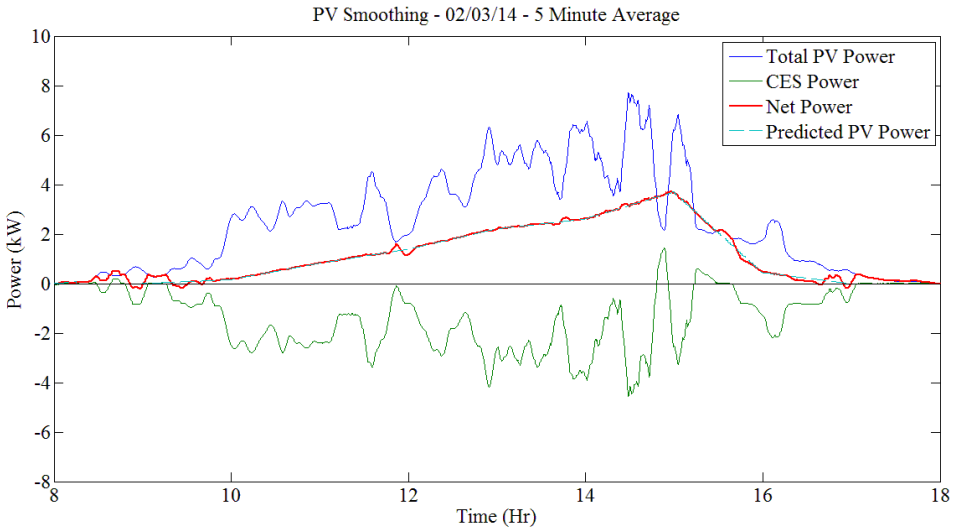

Figure A.18: Results from PV smoothing 02/03/2014 – 5 minute average

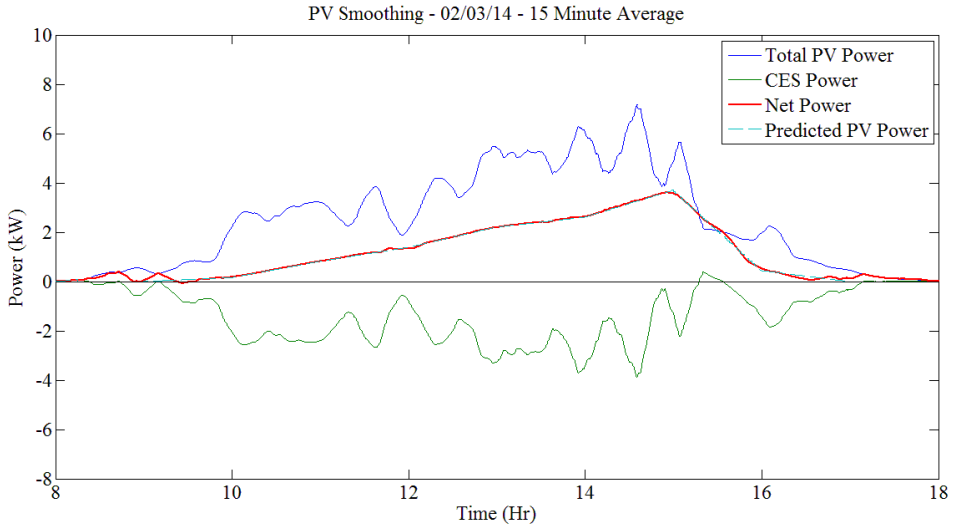

Figure A.19: Results from PV smoothing 02/03/2014 – 15 minute average

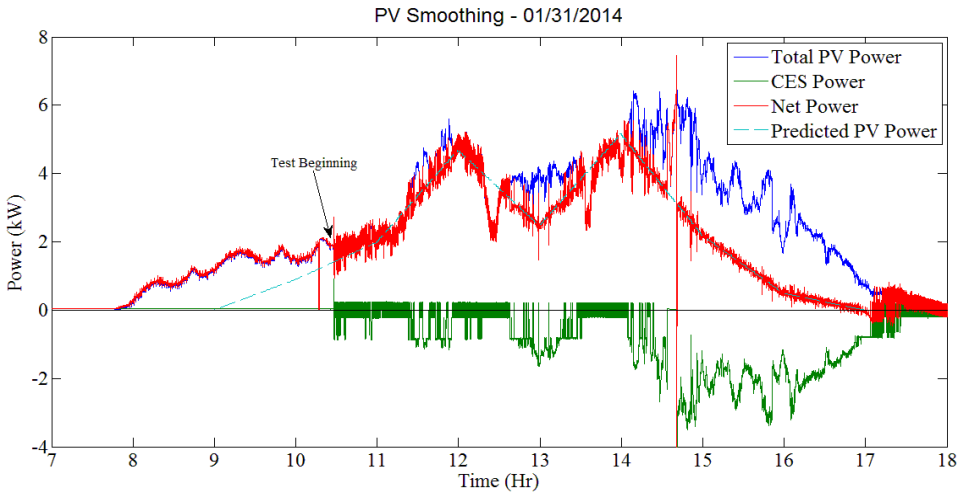

Figure A.20: Results from PV smoothing 01/31/2014 – no averaging

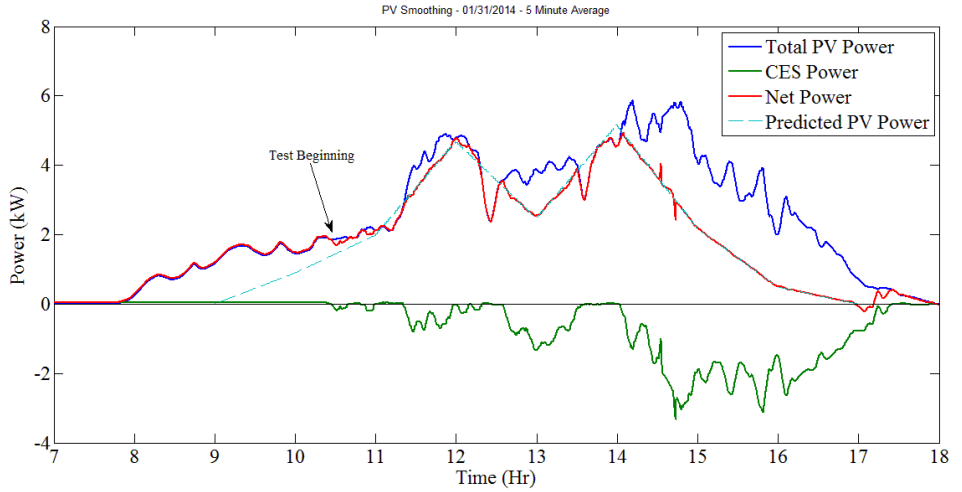

Figure A.21: Results from PV smoothing 01/31/2014 – 5 minute average

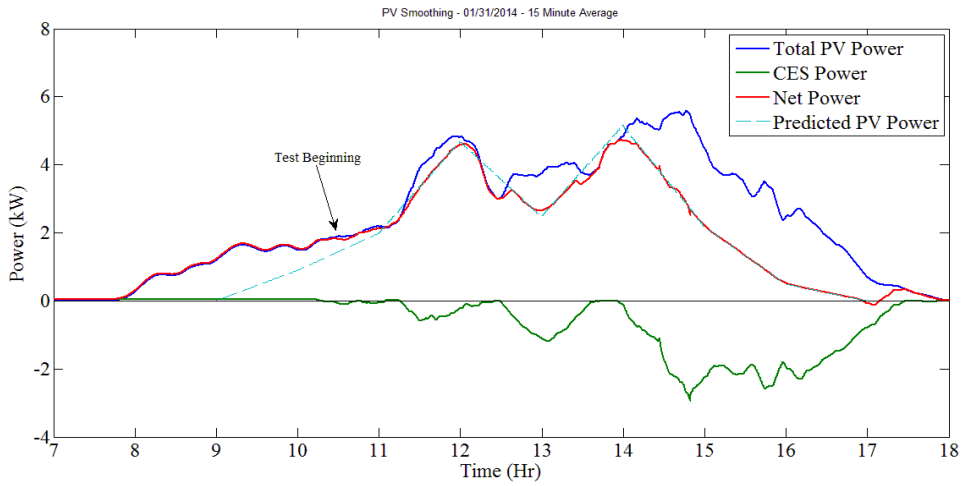

Figure A.22: Results from PV Smoothing 01/31/2014 – 15 minute average

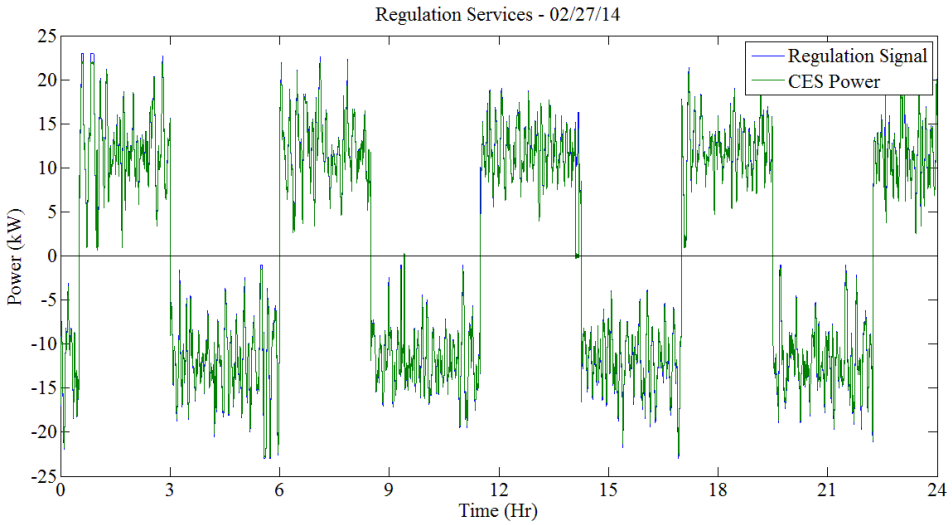

Figure A.23: Results from Figure 4.12 – no averaging

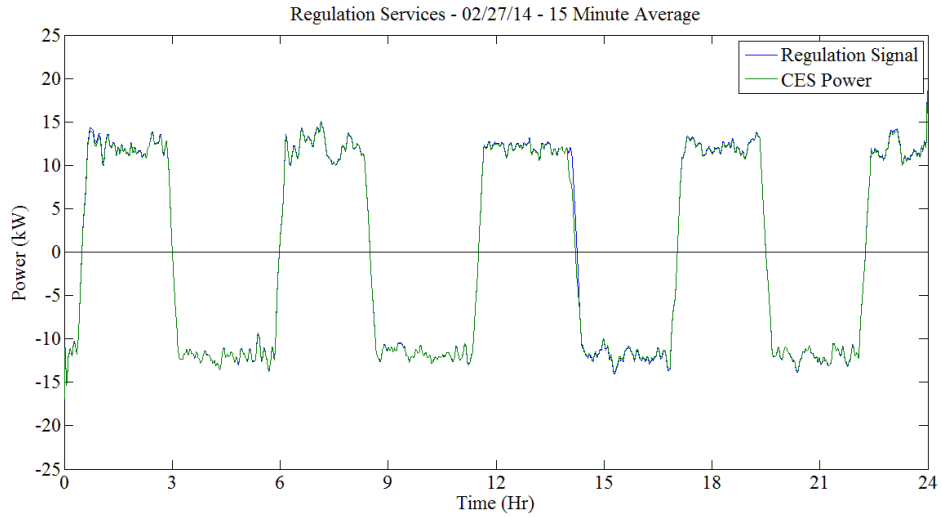

Figure A.24: Results from Figure 4.12 – 15 minute average

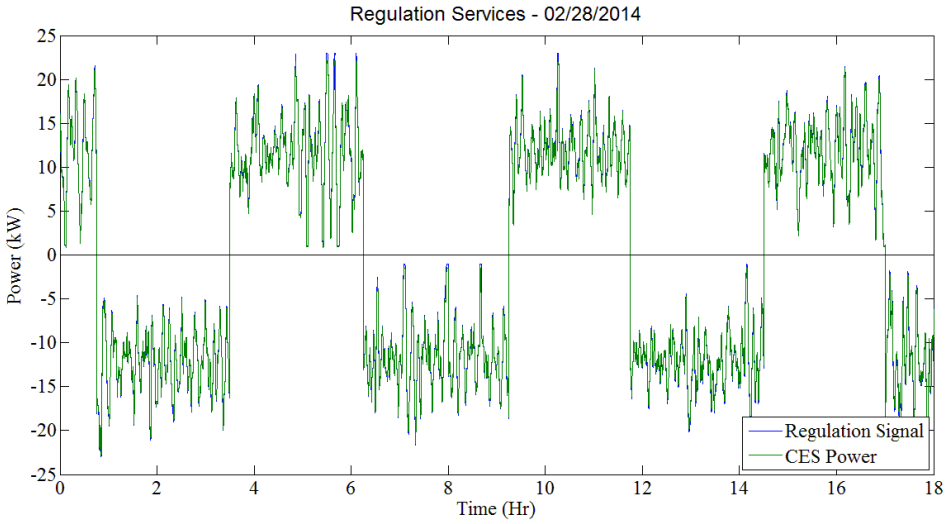

Figure A.25: Results from regulation services 02/28/2014 – no averaging

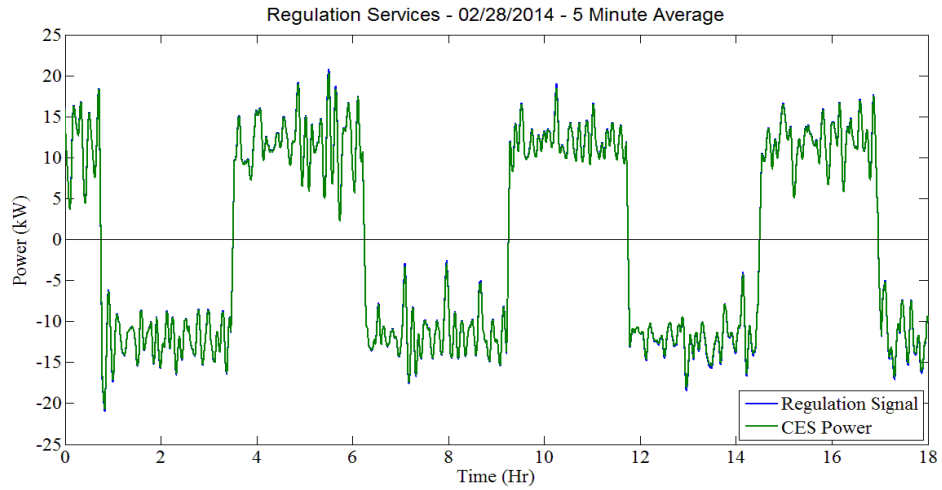

Figure A.26: Results from regulation services 02/28/2014 – 5 minute average

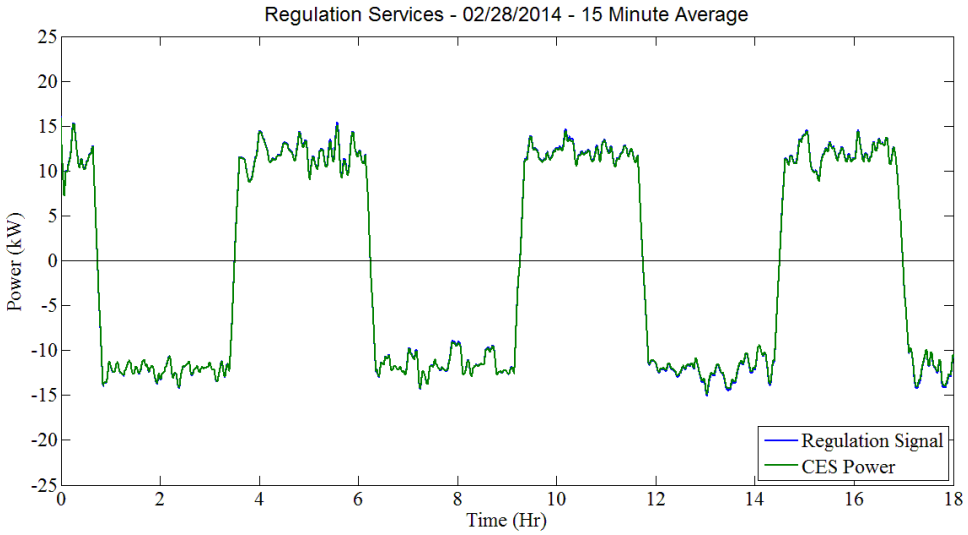

Figure A.27: Results from regulation services 02/28/2014 – 15 minute average

VITA

Ben Ollis was born in Clinton, Tennessee. He graduated from the University of Tennessee, Knoxville in December 2012 with a Bachelor of Science degree in Electrical Engineering. Ben continued his education by attending graduate school at the University of Tennessee, Knoxville, where he graduated in Spring 2014 with a Master of Science degree in Electrical Engineering with a concentration in Power Systems. During graduate school, Ben was a research assistant in the Power and Energy Systems group at Oak Ridge National Laboratory where he performed the research for this thesis. He plans to begin a career in the power and energy systems field.